THE JOURNAL OF BIOLOGICAL CHEMISTRY VOL. 285, NO. 38, pp. 29239–29246, September 17, 2010

Convergence of Ser/Thr and Two-component Signaling to Coordinate Expression of the Dormancy Regulon in *Mycobacterium tuberculosis*[*] [S]

Received for publication, April 11, 2010, and in revised form, July 12, 2010 Published, JBC Papers in Press, July 14, 2010, DOI 10.1074/jbc.M110.132894

Joseph D. Chao[‡1,2], Kadamba G. Papavinasasundaram[§1,3], Xingji Zheng[§], Ana Chávez-Steenbock[§], Xuetao Wang[§], Guinevere Q. Lee[§], and Yossef Av-Gay[‡§4]

From the [‡]Department of Microbiology and Immunology and the [§]Division of Infectious Diseases, Department of Medicine, University of British Columbia, Vancouver, British Columbia V5Z 3J5, Canada

Signal transduction in *Mycobacterium tuberculosis* is mediated primarily by the Ser/Thr protein kinases and the two-component systems. The Ser/Thr kinase PknH has been shown to regulate growth of *M. tuberculosis* in a mouse model and in response to NO stress *in vitro*. Comparison of a *pknH* deletion mutant (Δ*pknH*) with its parental *M. tuberculosis* H37Rv strain using iTRAQ enabled us to quantify >700 mycobacterial proteins. Among these, members of the hypoxia- and NO-inducible dormancy (DosR) regulon were disregulated in the Δ*pknH* mutant. Using kinase assays, protein-protein interactions, and mass spectrometry analysis, we demonstrated that the two-component response regulator DosR is a substrate of PknH. PknH phosphorylation of DosR mapped to Thr^{198} and Thr^{205} on the key regulatory helix α10 involved in activation and dimerization of DosR. PknH Thr phosphorylation and DosS Asp phosphorylation of DosR cooperatively enhanced DosR binding to cognate DNA sequences. Transcriptional analysis comparing Δ*pknH* and parental *M. tuberculosis* revealed that induction of the DosR regulon was subdued in the Δ*pknH* mutant in response to NO. Together, these results indicate that PknH phosphorylation of DosR is required for full induction of the DosR regulon and demonstrate convergence of the two major signal transduction systems for the first time in *M. tuberculosis*.

Mycobacterium tuberculosis, the causative agent of tuberculosis, is a human intracellular pathogen that is phagocytosed by alveolar macrophages and subsequently "walled off" by the host immune response within granulomas (1). *M. tuberculosis* is able to persist within the hostile microenvironment of the granuloma, which is thought to include hypoxic, acidic, and nutrient-poor conditions and immune effectors such as nitric oxide (NO)[5] (2). The survival and persistence of *M. tuberculosis* in this environment requires the ability to sense external signals and mount an effective adaptive response. *M. tuberculosis* possesses multiple families of signal transduction systems, including the Ser/Thr protein kinases (STPKs) and the two-component regulatory systems (TCSs) (3).

In a previous study, we found that the STPK PknH functions as an *in vivo* growth regulator (4). Hypervirulence was consistently detected in BALB/c mice infected with a *pknH* deletion mutant in *M. tuberculosis* after 3–4 weeks of infection (4), corresponding to the onset of adaptive immunity. Therefore, we hypothesized that *M. tuberculosis* uses the PknH kinase-mediated pathways to respond to host-induced signals to regulate its *in vivo* growth. Nitric oxide produced by the inducible nitric-oxide synthase of the host macrophages plays a key role in controlling bacillary growth during the chronic phase of infection following activation of the host immune response (5). *In vitro* experiments revealed that the Δ*pknH* mutant is more resistant to NO compared with WT (4), indicating that PknH may act as a sensor of NO to regulate *M. tuberculosis* growth *in vivo*.

Predictions from bioinformatics analysis and studies using *in vitro* kinase assays have identified three endogenous substrates of PknH kinase: EmbR (6), a transcriptional regulator of the *embCAB* genes involved in lipoarabinomannan and arabinogalactan synthesis; DacB1, a cell division-related protein; and Rv0681, a putative transcriptional regulator (7). However, the substrates and downstream effectors of PknH signaling in response to NO stimulus have yet to be discovered.

The DosR system, also known as DevR, is one of 11 pairs of TCSs present in *M. tuberculosis* (3). It is well established that DosR responds to hypoxia, NO, and CO via signaling through two cognate sensor kinases, DosS (DevS) and DosT (8, 9) to activate transcription of a defined set of ~50 genes termed the "dormancy" or DosR regulon (10). Genes belonging to the DosR regulon, including *dosR*, are up-regulated in the Wayne model of dormancy (10, 11), under low-oxygen tension (12–14), and in response to NO (10) and CO (15, 16) and are believed to be involved in the adaptation of *M. tuberculosis* to a non-replicating persistent state in latent tuberculosis infection.

* This work was supported in part by Canadian Institutes of Health Research Grant MOP-68857 (to Y. A.-G.) and the TB Veterans Charitable Foundation (to Y. A.-G.).

[S] The on-line version of this article (available at http://www.jbc.org) contains supplemental "Methods," Figs. S1–S3, and Tables S1 and S2.

[1] Both authors contributed equally to this work.

[2] Recipient of the Canadian Institutes of Health Research Canada Graduate Scholarships Doctoral Award.

[3] Present address: Dept. of Molecular Genetics and Microbiology, University of Massachusetts Medical School, Worcester, MA 01655.

[4] To whom correspondence should be addressed: Dept. of Medicine, University of British Columbia, 2733 Heather St., Vancouver, British Columbia V5Z 3J5, Canada. Tel.: 604-875-4329; Fax: 604-875-4013; E-mail: yossi@interchange.ubc.ca.

[5] The abbreviations used are: NO, nitric oxide; STPK, Ser/Thr protein kinase; TCS, two-component system; iTRAQ, isobaric tag for relative and absolute quantitation; qRT-PCR, quantitative real-time PCR; mDHFR, murine dihydrofolate reductase; CP, central and proximal; D, distal.

In this work, we demonstrate convergence of the two major signal transduction systems, the STPK and the TCS, for the first time in *M. tuberculosis*. Using a global proteomics approach, we identified members of the DosR regulon to be disregulated in a *pknH* deletion mutant in *M. tuberculosis*. We show that DosR is a substrate of PknH Thr phosphorylation and that cooperative DosS Asp phosphorylation and PknH Thr phosphorylation enhance DosR-DNA binding. Enhanced binding *in vitro* correlates with up-regulation of the DosR regulon in WT *M. tuberculosis* compared with Δ*pknH* in response to NO. These results suggest that PknH and the Dos TCS coordinately regulate expression of a key physiological response of *M. tuberculosis*.

EXPERIMENTAL PROCEDURES

M. tuberculosis Growth/Stress Conditions—*M. tuberculosis* H37Rv and a mutant strain lacking *pknH*, described previously (4), were grown in Middlebrook 7H9 broth supplemented with 10% albumin/dextrose/sodium chloride and 0.05% Tween 80. For iTRAQ analysis, strains were grown in rolling cultures to $A_{600} \approx 1.0$, harvested, washed, and resuspended in acidified (pH 5.4) Middlebrook 7H9 broth/Tween 80/albumin/dextrose/sodium chloride with 3.0 mM $NaNO_2$ and harvested after 48 h in standing cultures as described previously (4). For qRT-PCR analysis, cultures were grown in rolling cultures to $A_{600} \approx 0.3$ and treated for 4 h with $NaNO_2$ or diethylenetriamine/NO as indicated. Cells were washed and resuspended when using acidified media.

iTRAQ and LC-MS/MS—The iTRAQ assay and phosphopeptide identification were performed by the University of Victoria Proteomics Centre (British Columbia, Canada; see supplemental "Methods").

RNA Extraction and qRT-PCR—Previously described procedures were followed for RNA extraction and qRT-PCR analysis (4). Primers for qRT-PCR are listed in supplemental Table S1. Results were analyzed using GraphPad Prism software. All values were normalized to cDNA expression levels of *sigA*.

Cloning, Expression, and Purification—Plasmids and primers used for cloning and site-directed mutagenesis are listed in supplemental Table S1. The genes *pknH-(1–402)*, *dosR*, and *dosS-(378–578)* were amplified from *M. tuberculosis* H37Rv genomic DNA using standard methods. The *dosR* gene was cloned into the pET22b vector; *dosS-(378–578)* was cloned downstream of G-protein coding sequence into a modified pGEV2 vector (17), pJC8 (see supplemental "Methods"). Site-directed mutagenesis was performed as described previously (7). For cell-based phosphorylation experiments, *dosR* was transferred into the pET30b kanamycin-resistant vector (producing an identical DosR recombinant protein), *pknH* was cloned into the pGEX-4T3 ampicillin-resistant vector, and both were cotransformed into *Escherichia coli* BL21. Expression of all proteins was carried out in *E. coli* BL21(DE3) as described (7), followed by purification on nickel-nitrilotriacetic acid columns (Qiagen) according to the supplied protocol.

In Vitro Kinase Assays—*In vitro* kinase assays were carried out as described previously (7). For EMSA, PknH and DosS were autophosphorylated in 25 mM Tris-HCl (pH 7.5), 5 mM $MgCl_2$, 1 mM $MnCl_2$, 20 mM KCl, 1 mM DTT, and 1.0 mM unlabeled ATP.

Phosphoamino Acid Stability and Analysis—PknH-phosphorylated DosR was separated by SDS-PAGE and transferred onto 0.45-μm PVDF membranes. Stability of the incorporated phosphate was tested by treating membranes with 1 N HCl, 3 N NaOH, or ddH_2O overnight at room temperature and visualized by phosphorimaging. Phosphoamino acid analysis was performed as described (18) using cellulose plates and resolved in one dimension with isobutyric acid and 0.5 M NH_4OH (5:3, v/v).

Protein-Protein Interaction Assays—See supplemental Table S1 for primers and plasmids. The mycobacterial protein fragment complementation assay was performed as described (19). *M. tuberculosis dosR* and *pknH-(1–401)* genes were amplified by PCR and cloned into pUAB100 (expressing murine dihydrofolate reductase (mDHFR) fragment F1,2) and pUAB200 (expressing mDHFR fragment F3), producing pKP366 and pKP369, respectively. *Mycobacterium smegmatis* was cotransformed with both plasmids, and the cotransformants were selected on 7H11/kanamycin/hygromycin plates and tested for growth over 3–4 days on kanamycin/hygromycin plates supplemented with 0, 10, and 20 μg/ml trimethoprim.

The Trp auxotrophic strain of *M. smegmatis* and plasmids pL240 and pL242, containing the N- and C-terminal fragments (N_{Trp} and C_{Trp}) of *N*-(5′-phosphoribosyl)anthranilate isomerase, respectively, were generously provided by Helen O'Hare. The Split-Trp experiment was performed as described (20), with the following modifications. N_{Trp} and C_{Trp} were transferred from pL240 and pL242 into pALACE (21) and pPE207 (22) and designated pJC10 (hygromycin-resistant) and pJC11 (apramycin-resistant), respectively, to place the resulting fusion proteins under control of the inducible acetamidase promoter (see supplemental "Methods"). The indicated genes were PCR-amplified and cloned into pJC10 and pJC11. All inserts were sequenced. Cotransformed *M. smegmatis* Trp^- was spotted (5 μl) onto Middlebrook 7H10 broth, 1% glucose, 60 μg/ml histidine, 50 μg/ml hygromycin, and 30 μg/ml apramycin plates; supplemented or not with either 0.02% acetamide or 120 μg/ml Trp; and grown for 2–3 weeks at 30 °C.

EMSA—Oligonucleotides corresponding to the combined central and proximal (CP) DosR boxes and the distal (D) box upstream of *hspX* were designed with 5′-guanine overhangs when annealed (supplemental Table S1). Radioactive [α-^{32}P]dCTP was incorporated by Klenow (Fermentas) according to the supplied protocol. DosR (64 pmol) was phosphorylated by incubation with and without 0.2 μg each of pre-autophosphorylated PknH, DosS, and both PknH and DosS, followed by incubation with 4 pmol of radiolabeled CP or D DosR boxes. Binding conditions were as described previously (23). Samples were resolved by 5% nondenaturing Tris borate/EDTA PAGE. Gels were dried, and radiolabeled DNA bands were detected by phosphorimaging.

RESULTS

PknH-dependent Protein Expression—To draw a global picture of the regulation mediated by PknH kinase, we compared the protein expression profiles of WT and Δ*pknH M. tubercu-*

losis using the quantitative MS-based proteomics approach, iTRAQ (24). On the basis of our previous study showing that the Δ*pknH* mutant survives better than WT *M. tuberculosis* and the complemented strain in standing cultures treated with acidified nitrite ($NaNO_2$, an NO donor under acidic conditions) (4), we compared the global protein levels of the Δ*pknH* mutant and its WT parental strain with and without a 48-h $NaNO_2$ treatment. We were able to identify and simultaneously compare the expression of 784 proteins using a cutoff of 95% probability in the identification of peptides (supplemental Table S2). Of these, 447 proteins were identified using at least two high-confidence peptides (>95%). Of the 331 proteins identified with a single high-confidence peptide, 262 proteins were identified with at least a second unique peptide of lower confidence (<95%), resulting in a cumulative unused protein score of >2.0. In total, 706 proteins were identified with high confidence based on the unused protein score of >2.0 (see supplemental "Methods" for data analysis).

Fig. 1*A* shows the distribution of the Δ*pknH*/WT protein level ratios based on their chromosomal location. The ratios of individual protein levels ranged from 0.67 to 2.36 for untreated samples and from 0.58 to 1.97 for NO-treated samples. To identify proteins that differentially responded to NO through PknH signaling, we plotted the changes in protein expression due to NO treatment in Δ*pknH versus* WT (Δ*pknH*/Δ*pknH* + NO *versus* WT/WT + NO) (Fig. 1*B*). Grouping the data into four clusters using the *K*-mean clustering algorithm, we identified the cluster with the highest mean attribute value to contain nine proteins having greater levels in the Δ*pknH* mutant compared with WT and responding to NO treatment (Fig. 1*B*, *circled*). Strikingly, eight of the nine proteins are encoded within the DosR regulon. Further examination of the iTRAQ data revealed that of the 48 genes commonly regulated by DosR in response to NO, hypoxia, and the Wayne model of dormancy (10), 13 gene products were identified by iTRAQ, all of which had higher protein levels in the Δ*pknH* mutant after 48-h standing conditions (Table 1). With the addition of $NaNO_2$, these 13 DosR-regulated proteins were induced to similar levels in WT and Δ*pknH* (Table 1).

PknH Phosphorylation of DosR on Thr—As each of the 13 proteins identified displayed the same expression pattern in Δ*pknH* compared with WT, we reasoned that this pattern likely represents the entire DosR regulon and suggests that the mechanism of PknH regulation occurs at the level of the transcriptional regulator, DosR. The transcriptional activity of DosR is dependent on phosphorylation of Asp^{54} by its cognate histidine kinases, DosS and DosT, in response to hypoxia, NO, and CO (9, 12). However, on the basis of our data, we hypothesized that PknH kinase regulates DosR activity by Ser/Thr phosphorylation. We therefore conducted *in vitro* kinase assays to test whether PknH phosphorylates DosR. As shown in Fig. 2*A*, DosR was phosphorylated when incubated with recombinant PknH, whereas DosR alone did not undergo autophosphorylation.

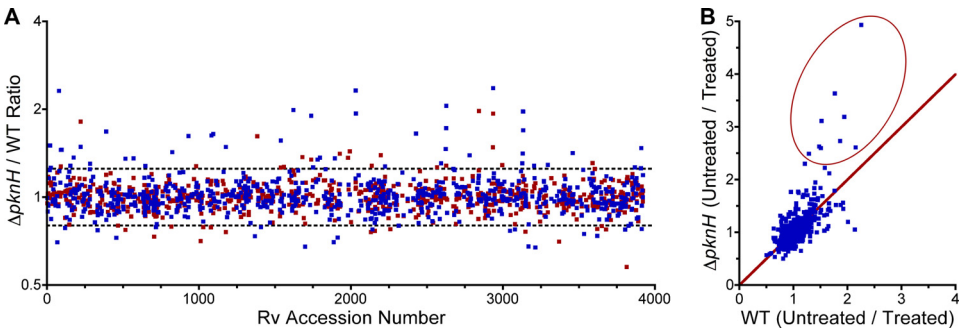

FIGURE 1. **Graphical analysis of iTRAQ ratios.** *A*, distribution of iTRAQ ratios based on Rv accession number (TubercuList). Using arbitrary cutoff values of 1.25 and 0.8, 47 proteins were up-regulated and 21 were down-regulated in the *pknH* mutant in the absence of NO stimulus, whereas 20 were up-regulated and 17 were down-regulated after treatment with NO. *Blue squares*, untreated Δ*pknH*/WT ratios; *red squares*, acidified nitrite-treated Δ*pknH*/WT ratios. *B*, scatter plot of untreated/acidified nitrite-treated ratios of Δ*pknH versus* WT. *Circled* points represent proteins that clustered with the highest mean attribute value based on *K*-mean clustering of data points; eight of the nine points represent proteins encoded in the DosR regulon.

TABLE 1

iTRAQ comparison of DosR-dependent protein levels

Ratios (Δ*pknH*/WT) of DosR-inducible proteins identified by iTRAQ analysis are shown for cultures with and without treatment with 3.0 mM acidified nitrite. In untreated samples, DosR-regulated proteins that are commonly induced by NO (10), hypoxia (12), and standing conditions (32) all had elevated levels in the Δ*pknH* mutant but approached ratios of 1.0 upon acidified nitrite treatment. This pattern of expression was not observed for proteins (Rv1177, Rv0231, and Rv3841) whose gene expression is DosR-dependent in response to hypoxia and standing conditions but not to NO. USPA, Universal Stress Protein A.

Gene	Function	Untreated ratio	NO-treated ratio	DosR-inducible Ref.
Rv0079	Hypothetical	2.31	1.04	(10, 12, 32)[a]
Rv1738	Conserved	1.90	1.35	(10, 12, 32)
Rv2030c	Conserved	1.16	1.07	(10, 12, 32)
Rv2031c (*hspX*)	α-Crystallin	2.32	1.12	(10, 12, 32)
Rv2032 (*acg*)	Conserved	1.93	1.08	(10, 12, 32)
Rv2623	USPA motif	1.46	1.16	(10, 12, 32)
Rv2626c	Conserved	1.72	1.28	(10, 12, 32)
Rv2627c	Conserved	2.05	0.99	(10, 12, 32)
Rv3127	Conserved	1.31	0.92	(10, 12, 32)
Rv3130c	Conserved	1.41	0.96	(10, 12, 32)
Rv3131	Conserved	1.97	1.18	(10, 12, 32)
Rv3133c (*dosR*)	TCS response regulator	1.69	1.05	(10, 12, 32)
Rv3134c	USPA motif	1.96	1.13	(10, 12, 32)
Rv1177 (*fdxC*)	Ferredoxin	1.49	0.76	(32)
Rv0231 (*fadE4*)	Acyl-CoA dehydrogenase	0.86	0.98	(32)
Rv3841 (*bfrB*)	Bacterioferritin	0.81	0.98	(12)

[a] Kendall *et al.* (32) identified Rv0080, which belongs to the same operon as Rv0079.

Phosphoamino acid analysis identified that DosR was phosphorylated on Thr (Fig. 2*B*). Phosphorylation was acid-stable and alkali-labile, characteristic of Thr phosphorylation, but not of Asp phosphorylation (supplemental Fig. S2) (25). MS/MS analysis identified PknH-monophosphorylated DosR at Thr^{198} (supplemental Fig. S1*A*) and Thr^{205} (supplemental Fig. S1*B*) of the trypsin-digested ^{198}TQAAVFATELKR^{209} peptide located in the C-terminal domain of DosR. Site-directed mutagenesis of DosR confirmed these findings: DosR(T198A) had reduced ability to be phosphorylated by PknH, and DosR(T205A) and DosR(T198A/T205A) were nearly abolished for PknH phosphorylation (Fig. 2*C*).

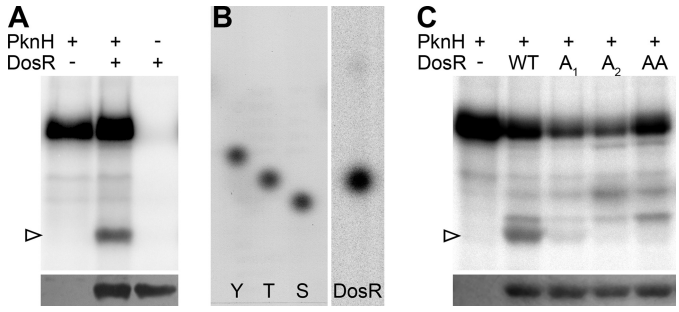

FIGURE 2. **PknH phosphorylation of DosR.** *A*, *in vitro* kinase assay demonstrated phosphorylation of DosR by PknH using [γ-^{32}P]ATP. *Upper*, phosphorimage; *lower*, silver stain of DosR protein bands. *B*, one-dimensional phosphoamino acid analysis of PknH-phosphorylated DosR identified phosphorylation on Thr. Control phospho-Tyr (*Y*), phospho-Thr (*T*), and phospho-Ser (*S*) were visualized by spraying with ninhydrin, and radiolabeled DosR residues were visualized by phosphorimaging. Retention factors were calculated as follows: Tyr, 0.37; Thr, 0.31; Ser, 0.25; and DosR, 0.30. *C*, *in vitro* kinase assay confirmed that DosR(T198A) (A_1), DosR(T205A) (A_2), and the double mutant DosR(T198A/T205A) (*AA*) are defective for phosphorylation by PknH. *Upper*, phosphorimage; *lower*, silver stain. *Arrowheads* point to DosR.

Next, we used *E. coli*, which lacks any known STPKs, as a surrogate host to test PknH phosphorylation of DosR in a cell-based system. The active kinase domain of PknH and full-length recombinant DosR were coexpressed in *E. coli*. MS/MS analysis of DosR purified from the PknH-expressing strain identified monophosphorylated (supplemental Fig. S1, *C* and *D*) and diphosphorylated (Fig. 3 and supplemental Fig. S1*E*) DosR at the previously identified Thr^{198} and Thr^{205} residues, with diphosphorylation being the predominant species.

PknH Interaction with DosR in Mycobacteria—To determine whether PknH interacts with DosR *in vivo*, we performed two separate protein-protein interaction assays in *M. smegmatis*: the Split-Trp assay (20) and mycobacterial protein fragment complementation assay (19). In the former, protein-protein interaction leads to the reassembly of the N- and C-terminal fragments (N_{Trp} and C_{Trp}) of *N*-(5′-phosphoribosyl)anthranilate isomerase, an enzyme required for Trp biosynthesis. In the

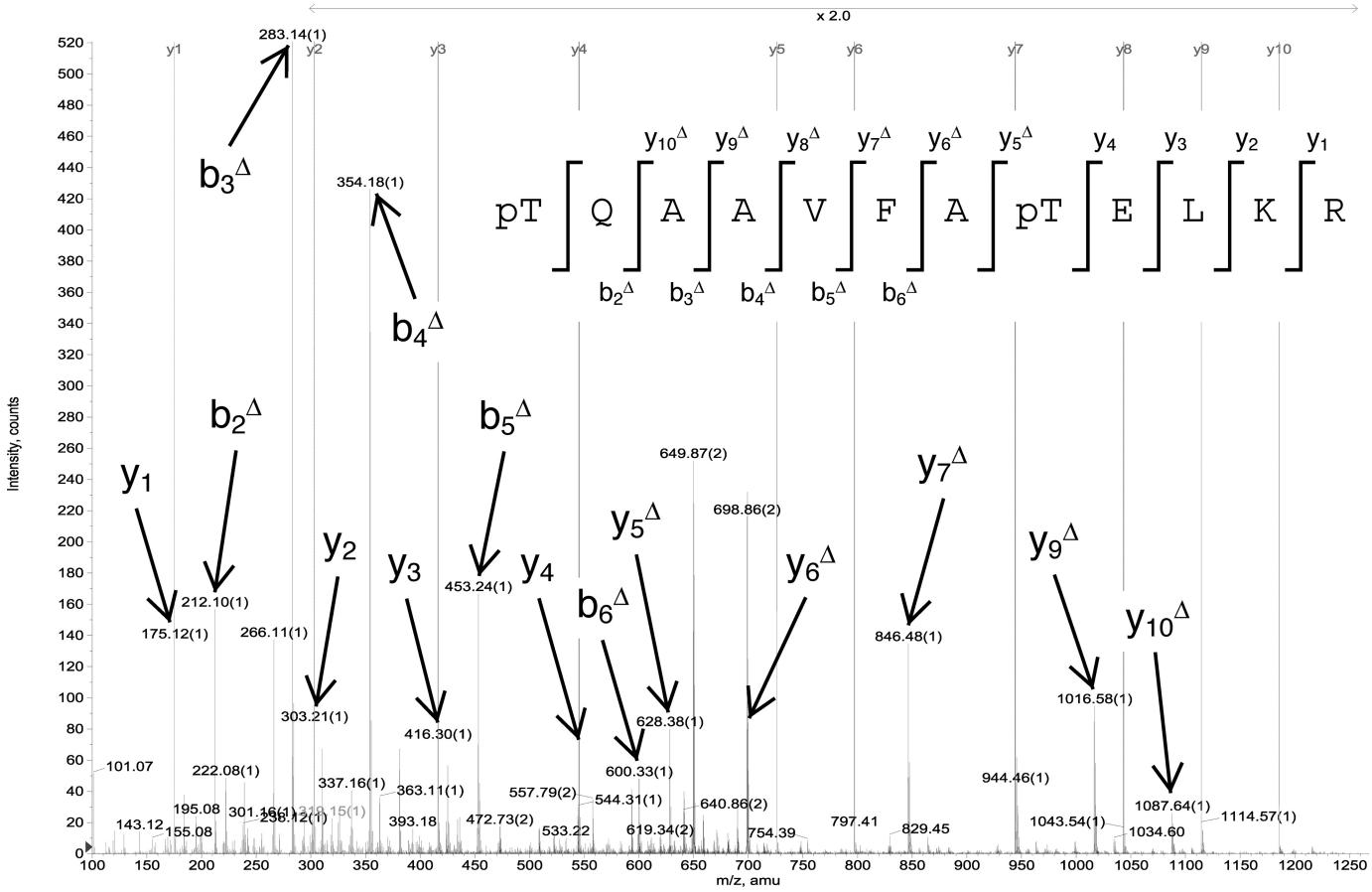

FIGURE 3. **Identification of DosR phosphorylation sites.** The MS/MS spectra represent peptide positions 198–209 with a monoisotopic mass of 1493.69 Da from DosR phosphorylated in a cell-based system showing diphosphorylation of Thr^{198} and Thr^{205}. Phosphorylation at Thr^{198} is shown by the b N-terminal daughter ion series, where all b ions identified lose phosphoric acid (−98 Da). Phosphorylation at Thr^{205} is shown by the y C-terminal daughter ion series, where all y ions after Thr^{205} lose phosphoric acid. *pT*, phosphothreonine; *amu*, atomic mass units.

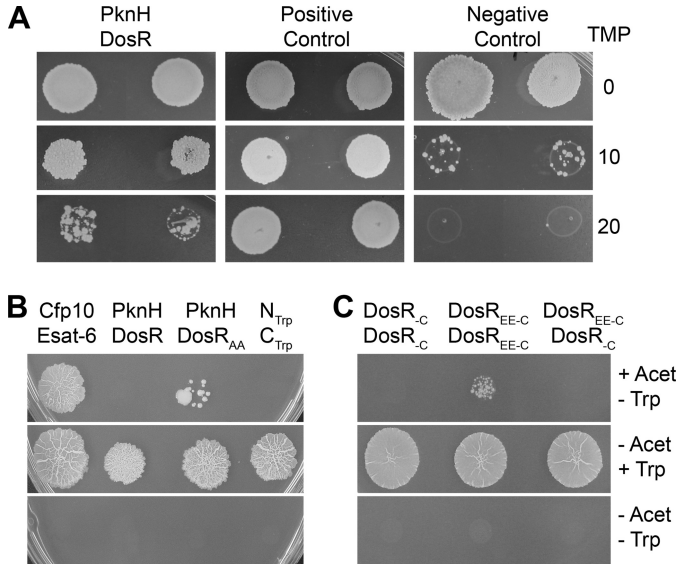

FIGURE 4. **PknH interaction with and dimerization of DosR *in vivo*.** *A*, PknH and DosR protein-protein interaction facilitated the reassembly of the F1,2 and F3 domains of mDHFR, enabling growth of *M. smegmatis* strains coexpressing DosR-F1,2 and PknH-(1–401)-F3 fusion proteins in the presence of 20 μg/ml trimethoprim (*TMP*). Identical spots on control plates without trimethoprim revealed growth of all strains. *Positive Control*, *Saccharomyces cerevisiae* Gcn4 dimerization domains fused to F1,2 and F3, respectively; *Negative Control*, mDHFR fragments alone. The experiment is shown in duplicate. *B*, the specific interaction between PknH and the phosphorylation-defective DosR(T198A/T205A) (*DosR$_{AA}$*) mutant facilitated the reassembly of the N_{Trp} and C_{Trp} fragments required for Trp biosynthesis, thus enabling growth of *M. smegmatis Trp*$^-$ strains coexpressing N_{Trp}-PknH-(1–401) with DosR(T198A/T205A)-C_{Trp}, but not with WT DosR-C_{Trp} (*upper row*). The positive control consisted of N_{Trp}-Cfp10 and Esat6-C_{Trp}. The negative control consisted of N_{Trp} and C_{Trp} alone. *C*, the growth of *M. smegmatis Trp*$^-$ was dependent on the reassembly of N_{Trp} and C_{Trp} mediated by the dimerization of the C-terminal domains (amino acids 145–217) of the phosphomimetic DosR(EE) mutant (*DosR$_{EE-C}$*), but not of WT DosR (*DosR$_{-C}$*) or the WT DosR/DosR(EE) (*DosR$_{-C}$*/*DosR$_{EE-C}$*) combination (*upper row*). *B* and *C*, *middle rows*, Trp supplied exogenously; *lower rows*, no acetamide (*Acet*) induction of the fusion proteins. Data are representative of three separate experiments.

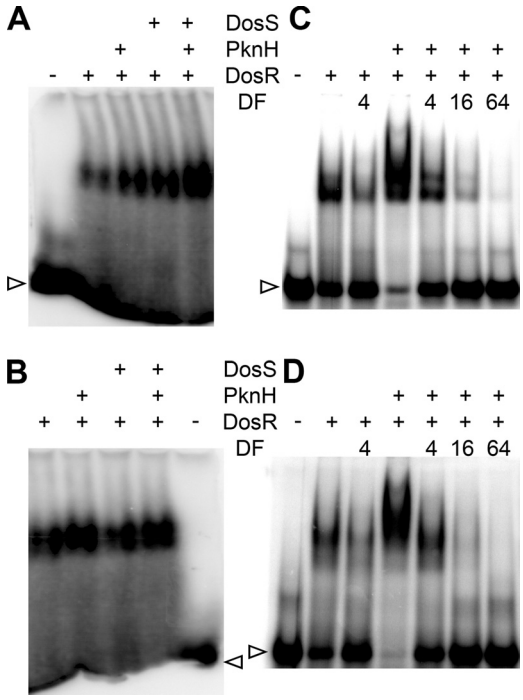

FIGURE 5. **Enhancement of DNA binding by PknH Thr-phosphorylated DosR.** Shown are phosphorimages of EMSA comparing the effects of Thr and Asp phosphorylation of DosR on the ability of DosR to bind the D and CP DosR boxes of the *hspX* promoter. *In vitro* phosphorylation of DosR by PknH and/or DosS increased binding to the D box (*A*) and CP box (*B*). Cell-based phosphorylation of DosR by PknH increased binding and caused an addition shift to the D box (*C*) and CP box (*D*). DosR was incubated with radiolabeled DNA and run on a nondenaturing gel. Radiolabeled DNA was titrated with excess unlabeled probe by the dilution factor (*DF*) indicated to show specific binding. *Arrowheads* show unbound DNA. Data are representative of three separate experiments.

latter, reassembly of complementary fragments F1,2 and F3 of mDHFR confers resistance to trimethoprim.

As shown in Fig. 4*A*, using the mycobacterial protein fragment complementation system, coexpression of DosR-F1,2 and PknH-(1–401)-F3 reconstituted mDHFR expression as determined by trimethoprim resistance, indicating that PknH interacts with DosR *in vivo*. The interaction between PknH and DosR in *M. smegmatis* was slightly weaker than the positive control obtained with the interaction of the yeast Gcn4 dimerization domains but is consistent with the transient nature of kinase-substrate interactions. Using the less sensitive Split-Trp system, interaction between PknH and WT DosR was not observed; however, interaction between PknH and the phosphorylation-defective DosR(T198A/T205A) mutant restored growth of the Trp auxotrophic strain of *M. smegmatis* in the absence of exogenous Trp (Fig. 4*B*). This result suggests that the PknH-DosR interaction is dependent on the phosphorylation status of DosR. DosR(T198A/T205A) likely acted as a kinase-trapping mutant, where PknH was able to bind but not release DosR(T198A/T205A) due to its inability to be phosphorylated. This result is in agreement with Split-Trp studies related to another *M. tuberculosis* protein kinase, PknG, which interacts significantly better with its phosphorylation-defective substrate, GarA(T21A), compared with WT GarA (26). Taken together, these results provide further evidence that PknH interacts with and phosphorylates DosR in mycobacteria.

Enhanced DNA Binding of PknH-phosphorylated DosR—DosR is able to bind its cognate DNA sequence, the DosR box (12), and Asp phosphorylation enhances DosR-DNA binding (27). We therefore assessed the effect of PknH on DosR-DNA binding using EMSA. We compared the DNA-binding ability of PknH Thr-phosphorylated DosR with unphosphorylated and DosS Asp-phosphorylated DosR. We tested the binding of DosR to the D and CP DosR boxes in the promoter region of *hspX*, a DosR regulon member that we found to be disregulated in the Δ*pknH* mutant. Thr phosphorylation of DosR by PknH enhanced binding of DosR to the D site of the *hsp*X promoter in a manner comparable with Asp phosphorylation of DosR by DosS (Fig. 5*A*). The binding of DosR to the D site was further enhanced by the combined phosphorylation of DosR by both PknH and DosS (Fig. 5*A*). In the absence of DosR, PknH did not cause a shift to the DNA (data not shown). PknH phosphorylation of DosR also enhanced binding of DosR to the CP site, although DosS phosphorylation of DosR did not affect DosR binding to this site (Fig. 5*B*). This latter result may suggest that DosR has different affinities for different DosR boxes, although the absence of enhanced binding may also be a result of DosS dephosphorylation of DosR, as DosS catalyzes this reverse reaction very shortly after Asp phosphorylation (28).

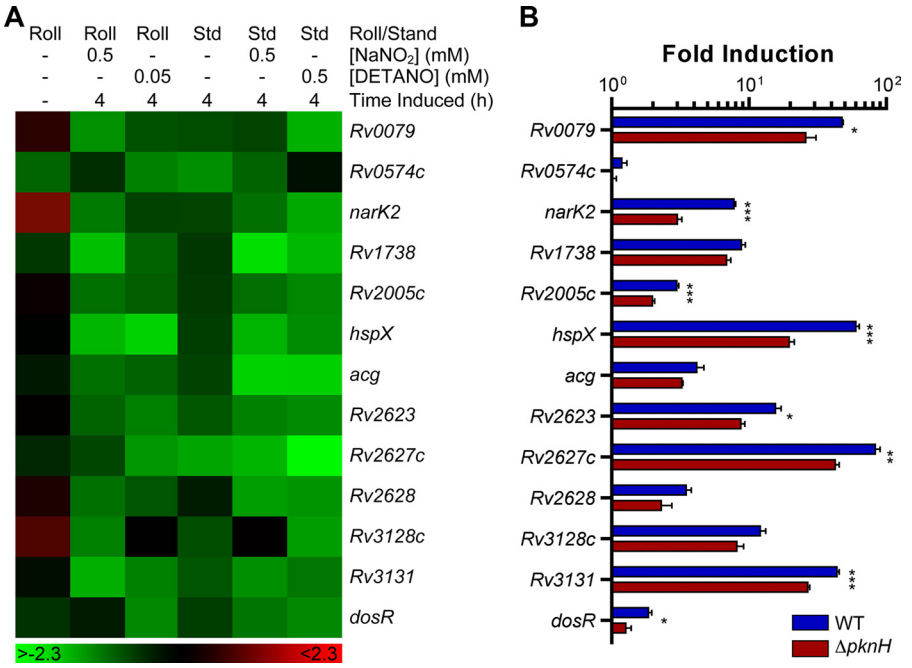

FIGURE 6. **Transcriptional analysis of DosR regulon genes in WT and Δ*pknH*.** *A*, heat map of qRT-PCR results showing Δ*pknH*/WT ratios for various culture conditions as indicated. Each gene was normalized to *sigA*. *Red* and *green spots* indicate greater or lesser gene expression in the Δ*pknH* mutant relative to WT *M. tuberculosis*, respectively. The *scale bar* indicates the mean of the $\log_2$ ratio. *B*, response of WT and the Δ*pknH* mutant to a 4-h treatment with 0.05 mM diethylenetriamine/NO (*DETANO*). Fold induction (±S.E.) was calculated by dividing gene expression levels in the treated cultures by the basal level expression in untreated cultures. *, $p < 0.05$; **, $p < 0.01$; ***, $p < 0.001$, significant difference compared with WT samples by Student's *t* test. *Std*, standing.

We also tested the DNA-binding characteristics of DosR that had been phosphorylated by PknH in our cell-based system. Equal amounts of DosR (as determined by Bradford assay and Coomassie Blue staining of gel-separated purified protein) were purified from *E. coli* with or without coexpression of PknH and used in the EMSA assay. As shown in Fig. 5 (*C* and *D*), cell-based phosphorylation of DosR by PknH not only resulted in a significantly more intense band but also caused an additional shift to both D and CP DosR boxes. These results indicate that PknH phosphorylation of DosR enhances its binding to cognate DNA sequences.

The C-terminal domain of DosR binds to its DNA sequences as a tetramer of two DosR dimers (29). As PknH phosphorylation enhanced DosR-DNA binding, we wanted to see if phosphorylation enhances DosR dimerization in mycobacteria using the Split-Trp method. Constant Thr phosphorylation was mimicked by mutating the two Thr phosphoacceptors of DosR to Glu (DosR(EE)) (30). As shown in Fig. 4*C*, interaction between the two C-terminal domains of the phosphomimetic DosR(EE) mutant restored growth of *M. smegmatis* Trp^-, whereas interaction between WT DosR proteins did not enable growth. Growth was not observed with either full-length WT or DosR(EE) proteins (data not shown) and was expected, as full-length DosR exists in an inactive conformation (31).

Transcription Profiling of the DosR Regulon in M. tuberculosis—As we observed greater DosR-DNA binding upon phosphorylation of DosR by PknH, we hypothesized that this increase in DNA binding would correlate to increased DosR regulon transcription in *M. tuberculosis*. We therefore used qRT-PCR to measure DosR regulon expression in WT *M. tuberculosis* compared with Δ*pknH*. For a broad coverage of the DosR regulon spanning the *M. tuberculosis* genome, we looked at the expression of eight DosR regulon genes whose products were identified in our iTRAQ analysis and five additional DosR regulon genes not identified by iTRAQ. All values were normalized to the housekeeping *sigA* gene, whose expression is affected neither by NO stress (32) nor by acidic conditions (33).

A heat map of the Δ*pknH*/WT ratios normalized to *sigA* expression for all 13 genes tested is shown in Fig. 6*A* (for graphical analysis, see supplemental Fig. S3). Basal level transcription of the DosR regulon in aerobic early log phase growth was unaffected by *pknH* deletion (*first column*). The addition of $NaNO_2$ resulted in an ~2-fold lower expression of the DosR regulon genes in Δ*pknH* compared with WT *M. tuberculosis* (*second column*). Because $NaNO_2$ can also generate reactive oxygen intermediates, we verified these results using diethylenetriamine/NO, a specific NO donor, and found a similar 2-fold decrease in DosR regulon expression in Δ*pknH* (*third column*). Expression of the regulon under standing conditions was also lower in the mutant, but to a lesser extent (*fourth column*). Finally, to mimic the combined low oxygen and presence of NO likely encountered in the host, standing conditions with the NO donors were tested and resulted in a similar decrease to DosR regulon expression in Δ*pknH* (*fifth* and *sixth columns*).

The decreased DosR regulon expression in the *pknH* mutant was due to an impaired induction of each gene following NO treatment (Fig. 6*B*). Comparison of gene expression in cultures treated with NO relative to basal level transcription revealed strong induction of the DosR regulon in WT *M. tuberculosis* (mean of 22.5-fold, maximum of 83.0-fold) but weaker induction in the Δ*pknH* mutant (mean of 11.6-fold, maximum of 42.4-fold) (Fig. 6*B*). Although this ~2-fold difference is relatively moderate, it is comparable with the 40–60% impaired induction observed in single knock-out mutants of DosS and DosT under hypoxic conditions (27, 34). The modest expression may also be due to compensating function(s) of other STPKs present in Δ*pknH M. tuberculosis*, as many of the STPKs appear to have substantial cross-talk activity (35). Nevertheless, these results indicate that PknH is required for full induction of the DosR regulon and agree with our EMSA analysis, suggesting that enhanced DNA binding of jointly Asp- and Thr-phosphorylated DosR leads to an increase in transcription of the regulon.

DISCUSSION

In this study, we have demonstrated for the first time that the dormancy regulon, an important and major regulatory response in the human pathogen *M. tuberculosis*, is controlled by two distinct signal transduction systems, the STPK and the TCS. We have shown that DosR is a substrate of PknH phosphorylation *in vitro* and in multiple cell-based systems. We also provide evidence that PknH phosphorylation of DosR enhances DosR dimerization and DNA binding, resulting in up-regulation of the DosR regulon in response to NO. A correlation between PknH and DosR has been suggested previously (36), and in this study, we provide the experimental basis to support this hypothesis.

Integration of these two types of signaling systems has been reported in other biological systems. In *Streptococcus agalactiae*, the STPK Stk1 phosphorylates the two-component response regulator CovR to repress CovR-dependent transcription of a secreted cytotoxin and to impede CovR transcriptional repression of a β-hemolysin/cytolysin gene (37) by inhibiting CovR-DNA binding (38). In *Myxococcus xanthus*, STPKs and a TCS coordinately regulate developmental changes in response to nutrient depletion. Expression of *mrpC*, encoding a transcription factor involved in fruiting body and myxospore formation, is transcribed by the TCS MrpAB but inhibited by Ser/Thr phosphorylation by the Pkn8/Pkn14 STPK cascade (39, 40). Convergence of STPKs and TCSs is also seen in eukaryotes where TCSs regulate activation of MAPK (Ser/Thr) signaling (41–43). Intriguingly, the HstK protein from the nitrogen-fixing *Anabaena* sp. PCC 7120 (44) and the NTHK2 ethylene receptor in tobacco plants (45) possess both Ser/Thr and histidine kinase activity. These examples demonstrate that STPKs and TCSs can be coupled to control a common signal transduction pathway.

Although further experiments are needed to elucidate the mechanism of action of PknH, the position of PknH phosphorylation suggests a potential means of post-translational regulation. Both phospho-Thr^{198} and phospho-Thr^{205} map to the critical regulatory helix α10 in the crystal structure of DosR (31). As suggested by Wisedchaisri *et al.* (31), DosR activation is dependent on the flexibility of this helix. In their model, helix α10 is in dynamic equilibrium in the closed-inactive conformation, bound to the N-terminal regulatory domain, burying the key Asp^{54} residue, and in an open-inactive conformation, allowing Asp^{54} to be solvent-exposed part of the time and thus available for Asp phosphorylation by DosS/T. Upon activation by Asp phosphorylation, helix α10 provides the DosR dimerization interface in an open-active conformation for DNA binding. Phosphorylation of helix α10 by PknH could potentially shift the equilibrium toward the open-inactive conformation of DosR, allowing for more efficient phosphorylation by DosS/T and activation of DosR. Alternatively, DosS/T phosphorylation may initiate conformational changes leading to the open-active conformation of DosR, whereas PknH phosphorylation may play a role in DosR dimerization.

Integration of PknH and DosS/T signal transduction systems controlling DosR activity would allow for tighter control of DosR-dependent activity. Activation of DosR by its cognate histidine kinases, DosS and DosT, results in a strong induction of the DosR regulon (27), and this induction is believed to be involved in metabolic changes that result in the pathogen entering a non-replicating persistent state. It is reasonable to expect mechanisms to be in place to prevent the pathogen from entering non-replicating persistence in the absence of an appropriate signal. Furthermore, nonspecific transcription and translation of the ~50 genes encoded in the DosR regulon would be considerably energy-costly. As a required second trigger (in addition to DosS/T) for full induction of the DosR regulon, PknH acts as a "molecular modulator" to repress nonspecific induction of the regulon and as an amplifier of the regulon in the presence of an appropriate signal.

The global proteomics approach proved to be a powerful tool for identifying key components in the PknH signal transduction pathway. However, our transcriptomic results seemingly contradict our proteomic data. The iTRAQ experiment was designed based on the enhanced survival of the *pknH* mutant in stationary phase growth exposed to lethal quantities of $NaNO_2$ (4) and was not designed to test specific DosR induction conditions. Furthermore, the 48-h time point tested in the iTRAQ experiment was well beyond the short-lived induction of the DosR regulon, whose gene expression largely returns to base line by 24 h (10, 46). Therefore, due to the difference in conditions and time points tested, the iTRAQ and qRT-PCR data cannot be directly compared. The somewhat discrepant results may indicate, however, that PknH also plays a role in inhibiting or turning off DosR regulon expression beyond the 24-h induction period. Further experiments, including a time-dependent analysis of DosR regulon expression under controlled conditions, would be required to test this hypothesis.

Deletion of *pknH* results in hypervirulence after 3–4 weeks of infection (4), corresponding to the induction of the host adaptive immune response and production of NO (47). It is tempting to speculate that the hypervirulence observed in the Δ*pknH* mutant may be mediated via signaling though DosR. An initial report indicated that deletion of *dosR* results in hypervirulence in mouse models (48). However, subsequent studies indicated that Δ*dosR* displays either attenuation or no difference in pathogenicity in mice, guinea pigs, and rabbits compared with WT *M. tuberculosis* (46, 49–51). Curiously, deletion of at least two members of the DosR regulon, *hspX* and Rv2623, each results in hypervirulence in mice (52, 53). Up-regulation of the DosR regulon has also been associated with hypervirulence, as genes belonging to the DosR regulon are constitutively up-regulated in the hypervirulent W-Beijing lineage of *M. tuberculosis* (54). It therefore remains a challenge to identify whether PknH signaling through DosR and/or the other known substrates contributes to the growth regulation and adaptation during the chronic or latent phase of infection.

Acknowledgments—We thank the British Columbia Centre for Disease Control for providing access to a Containment Level 3 facility; Derek Smith (University of Victoria Proteomics Centre) for iTRAQ and MS/MS experiments; Helen O'Hare for providing the Split-Trp system; and Mary Ko, Dennis Wong, and Amy Chao for technical assistance.

REFERENCES

1. Russell, D. G. (2007) *Nat. Rev.* **5,** 39–47
2. Rustad, T. R., Sherrid, A. M., Minch, K. J., and Sherman, D. R. (2009) *Cell. Microbiol.* **11,** 1151–1159
3. Av-Gay, Y., and Deretic, V. (2004) in *Tuberculosis and the Tubercle Bacillus* (Cole, S. T., Eisenach, K. D., McMurray, D. N., and Jacobs, W. R., eds) pp. 359–367, ASM Press, Washington, DC
4. Papavinasasundaram, K. G., Chan, B., Chung, J. H., Colston, M. J., Davis, E. O., and Av-Gay, Y. (2005) *J. Bacteriol.* **187,** 5751–5760
5. Flynn, J. L., and Chan, J. (2001) *Annu. Rev. Immunol.* **19,** 93–129
6. Molle, V., Kremer, L., Girard-Blanc, C., Besra, G. S., Cozzone, A. J., and Prost, J. F. (2003) *Biochemistry* **42,** 15300–15309
7. Zheng, X., Papavinasasundaram, K. G., and Av-Gay, Y. (2007) *Biochem. Biophys. Res. Commun.* **355,** 162–168
8. Saini, D. K., Malhotra, V., and Tyagi, J. S. (2004) *FEBS Lett.* **565,** 75–80
9. Kumar, A., Toledo, J. C., Patel, R. P., Lancaster, J. R., Jr., and Steyn, A. J. (2007) *Proc. Natl. Acad. Sci. U.S.A.* **104,** 11568–11573
10. Voskuil, M. I., Schnappinger, D., Visconti, K. C., Harrell, M. I., Dolganov, G. M., Sherman, D. R., and Schoolnik, G. K. (2003) *J. Exp. Med.* **198,** 705–713
11. Boon, C., Li, R., Qi, R., and Dick, T. (2001) *J. Bacteriol.* **183,** 2672–2676
12. Park, H. D., Guinn, K. M., Harrell, M. I., Liao, R., Voskuil, M. I., Tompa, M., Schoolnik, G. K., and Sherman, D. R. (2003) *Mol. Microbiol.* **48,** 833–843
13. Rosenkrands, I., Slayden, R. A., Crawford, J., Aagaard, C., Barry, C. E., 3rd, and Andersen, P. (2002) *J. Bacteriol.* **184,** 3485–3491
14. Sherman, D. R., Voskuil, M., Schnappinger, D., Liao, R., Harrell, M. I., and Schoolnik, G. K. (2001) *Proc. Natl. Acad. Sci. U.S.A.* **98,** 7534–7539
15. Shiloh, M. U., Manzanillo, P., and Cox, J. S. (2008) *Cell Host Microbe* **3,** 323–330
16. Kumar, A., Deshane, J. S., Crossman, D. K., Bolisetty, S., Yan, B. S., Kramnik, I., Agarwal, A., and Steyn, A. J. (2008) *J. Biol. Chem.* **283,** 18032–18039
17. Huth, J. R., Bewley, C. A., Jackson, B. M., Hinnebusch, A. G., Clore, G. M., and Gronenborn, A. M. (1997) *Protein Sci.* **6,** 2359–2364
18. Bach, H., Papavinasasundaram, K. G., Wong, D., Hmama, Z., and Av-Gay, Y. (2008) *Cell Host Microbe* **3,** 316–322
19. Singh, A., Mai, D., Kumar, A., and Steyn, A. J. (2006) *Proc. Natl. Acad. Sci. U.S.A.* **103,** 11346–11351
20. O'Hare, H., Juillerat, A., Dianisková, P., and Johnsson, K. (2008) *J. Microbiol. Methods* **73,** 79–84
21. Newton, G. L., Koledin, T., Gorovitz, B., Rawat, M., Fahey, R. C., and Av-Gay, Y. (2003) *J. Bacteriol.* **185,** 3476–3479
22. Paget, E., and Davies, J. (1996) *J. Bacteriol.* **178,** 6357–6360
23. Chauhan, S., and Tyagi, J. S. (2008) *J. Bacteriol.* **190,** 5394–5403
24. Ross, P. L., Huang, Y. N., Marchese, J. N., Williamson, B., Parker, K., Hattan, S., Khainovski, N., Pillai, S., Dey, S., Daniels, S., Purkayastha, S., Juhasz, P., Martin, S., Bartlet-Jones, M., He, F., Jacobson, A., and Pappin, D. J. (2004) *Mol. Cell. Proteomics* **3,** 1154–1169
25. Sickmann, A., and Meyer, H. E. (2001) *Proteomics* **1,** 200–206
26. O'Hare, H. M., Durán, R., Cerveñansky, C., Bellinzoni, M., Wehenkel, A. M., Pritsch, O., Obal, G., Baumgartner, J., Vialaret, J., Johnsson, K., and Alzari, P. M. (2008) *Mol. Microbiol.* **70,** 1408–1423
27. Roberts, D. M., Liao, R. P., Wisedchaisri, G., Hol, W. G., and Sherman, D. R. (2004) *J. Biol. Chem.* **279,** 23082–23087
28. Saini, D. K., Malhotra, V., Dey, D., Pant, N., Das, T. K., and Tyagi, J. S. (2004) *Microbiology* **150,** 865–875
29. Wisedchaisri, G., Wu, M., Rice, A. E., Roberts, D. M., Sherman, D. R., and Hol, W. G. (2005) *J. Mol. Biol.* **354,** 630–641
30. Kang, C. M., Nyayapathy, S., Lee, J. Y., Suh, J. W., and Husson, R. N. (2008) *Microbiology* **154,** 725–735
31. Wisedchaisri, G., Wu, M., Sherman, D. R., and Hol, W. G. (2008) *J. Mol. Biol.* **378,** 227–242
32. Kendall, S. L., Movahedzadeh, F., Rison, S. C., Wernisch, L., Parish, T., Duncan, K., Betts, J. C., and Stoker, N. G. (2004) *Tuberculosis* **84,** 247–255
33. Manganelli, R., Dubnau, E., Tyagi, S., Kramer, F. R., and Smith, I. (1999) *Mol. Microbiol.* **31,** 715–724
34. Honaker, R. W., Leistikow, R. L., Bartek, I. L., and Voskuil, M. I. (2009) *Infect. Immun.* **77,** 3258–3263
35. Prisic, S., Dankwa, S., Schwartz, D., Chou, M. F., Locasale, J. W., Kang, C. M., Bemis, G., Church, G. M., Steen, H., and Husson, R. N. (2010) *Proc. Natl. Acad. Sci. U.S.A.* **107,** 7521–7526
36. Greenstein, A. E., Grundner, C., Echols, N., Gay, L. M., Lombana, T. N., Miecskowski, C. A., Pullen, K. E., Sung, P. Y., and Alber, T. (2005) *J. Mol. Microbiol. Biotechnol.* **9,** 167–181
37. Rajagopal, L., Clancy, A., and Rubens, C. E. (2003) *J. Biol. Chem.* **278,** 14429–14441
38. Lin, W. J., Walthers, D., Connelly, J. E., Burnside, K., Jewell, K. A., Kenney, L. J., and Rajagopal, L. (2009) *Mol. Microbiol.* **71,** 1477–1495
39. Nariya, H., and Inouye, S. (2005) *Mol. Microbiol.* **58,** 367–379
40. Nariya, H., and Inouye, S. (2006) *Mol. Microbiol.* **60,** 1205–1217
41. Maeda, T., Wurgler-Murphy, S. M., and Saito, H. (1994) *Nature* **369,** 242–245
42. Posas, F., and Saito, H. (1998) *EMBO J.* **17,** 1385–1394
43. Stepanova, A. N., and Alonso, J. M. (2005) *Sci. STKE* **2005,** cm4
44. Phalip, V., Li, J. H., and Zhang, C. C. (2001) *Biochem. J.* **360,** 639–644
45. Zhang, Z. G., Zhou, H. L., Chen, T., Gong, Y., Cao, W. H., Wang, Y. J., Zhang, J. S., and Chen, S. Y. (2004) *Plant Physiol.* **136,** 2971–2981
46. Rustad, T. R., Harrell, M. I., Liao, R., and Sherman, D. R. (2008) *PLoS ONE* **3,** e1502
47. Shi, L., Jung, Y. J., Tyagi, S., Gennaro, M. L., and North, R. J. (2003) *Proc. Natl. Acad. Sci. U.S.A.* **100,** 241–246
48. Parish, T., Smith, D. A., Kendall, S., Casali, N., Bancroft, G. J., and Stoker, N. G. (2003) *Infect. Immun.* **71,** 1134–1140
49. Bartek, I. L., Rutherford, R., Gruppo, V., Morton, R. A., Morris, R. P., Klein, M. R., Visconti, K. C., Ryan, G. J., Schoolnik, G. K., Lenaerts, A., and Voskuil, M. I. (2009) *Tuberculosis* **89,** 310–316
50. Malhotra, V., Sharma, D., Ramanathan, V. D., Shakila, H., Saini, D. K., Chakravorty, S., Das, T. K., Li, Q., Silver, R. F., Narayanan, P. R., and Tyagi, J. S. (2004) *FEMS Microbiol. Lett.* **231,** 237–245
51. Converse, P. J., Karakousis, P. C., Klinkenberg, L. G., Kesavan, A. K., Ly, L. H., Allen, S. S., Grosset, J. H., Jain, S. K., Lamichhane, G., Manabe, Y. C., McMurray, D. N., Nuermberger, E. L., and Bishai, W. R. (2009) *Infect. Immun.* **77,** 1230–1237
52. Hu, Y., Movahedzadeh, F., Stoker, N. G., and Coates, A. R. (2006) *Infect. Immun.* **74,** 861–868
53. Drumm, J. E., Mi, K., Bilder, P., Sun, M., Lim, J., Bielefeldt-Ohmann, H., Basaraba, R., So, M., Zhu, G., Tufariello, J. M., Izzo, A. A., Orme, I. M., Almo, S. C., Leyh, T. S., and Chan, J. (2009) *PLoS Pathog.* **5,** e1000460
54. Reed, M. B., Gagneux, S., Deriemer, K., Small, P. M., and Barry, C. E., 3rd (2007) *J. Bacteriol.* **189,** 2583–2589

Supplemental Materials for

Convergence of Ser/Thr and Two-Component Signaling to Coordinate Expression of the Dormancy Regulon in *Mycobacterium tuberculosis*

Joseph D. Chao, K.G. Papavinasasundaram, Xingji Zheng, Ana Chávez-Steenbock, Xuetao Wang, Guinevere Q. Lee, and Yossef Av-Gay

This file includes:

SUPPLEMENTAL METHODS

iTRAQ analysis – The iTRAQ (Isobaric Tags for Related and Absolute Quantitation) strategy uses multiplexed set of reagents for quantitative protein analysis by placing isobaric mass labels at the N-termini and lysine side chains of peptides in a peptide mixture. Protein concentrations of WT and Δ*pknH* cell extracts were determined, and 100 μg of each protein sample in Dissolution buffer (Applied Biosystems) was denatured and treated with a reducing reagent at 60^{o}C for 1h. Cysteines in the proteins were blocked using a cysteine blocking reagent (Applied Biosystems) as described in the supplier's protocol. Each sample was digested with trypsin at 37 ^{o}C overnight and labeled with iTRAQ reagents 114-117 at room temperature for 1h. The labeled samples were then pooled and acidified in a total volume of 2.0 ml of Buffer A (10 mM KH_2PO_4 pH 2.7 and 25% acetonitrile (ACN)) and subjected to strong cation exchange (SCX) chromatography. The samples were injected onto a SCX column (Vision workstation (AB, Foster City, USA) equipped with Polysulfoethyl A (Poly LC, Columbia, MD) 100mm X 4.6mm, 5μM, 300Å SCX column). The column was allowed to equilibrate for 20 min in Buffer A before a gradient was applied; 0-35% Buffer B (10 mM KH_2PO_4, 25% ACN, 0.5M KCl) in 30 min. The flow rate was set at 0.5 mL/min. Fractions were collected every minute after injection and the samples were subjected to Speed-Vac drying to reduce the volume and transferred to autosampler vials (LC Packings, Amsterdam).

LC-MS/MS analysis – LC-MS/MS analysis was performed using an integrated Famos autosampler, Switchos II switching pump, and UltiMate micro pump system (LC Packings, Amsterdam) with a hybrid Quadrupole-TOF LC/MS/MS Mass Spectrometer (QStar Pulsar i) equipped with a nano-electrospray ionization source (Proxeon, Odense, Denmark) and fitted with a 10 μm fused-silica emitter tip (New Objective, Woburn, MA). Chromatographic separation was achieved on a 75μm x 15cm C18 PepMap Nano LC column (3μm, 100Å, LC Packings, Amsterdam) and a 300μm x 5mm C18 PepMap

guard column (5μm, 100Å, LC Packings, Amsterdam) was in place before switching inline with the analytical column and the MS. The mobile phase (solvent A) consisted of water/ACN (98:2 (v/v)) with 0.05% formic acid for sample injection and equilibration on the guard column at a flow rate of 100μL/min. A linear gradient was created upon switching the trapping column inline by mixing with solvent B, which consisted of ACN/water (98:2 (v/v) with 0.05% formic acid, and the flow rate was reduced to 200nL/min for high-resolution chromatography and introduction into the mass spectrometer.

Samples were brought up to 20μL with 5% ACN and 3% formaldehyde and transferred to autosampler vials (LC Packings, Amsterdam). Samples (10uL) were injected in 95% solvent A and allowed to equilibrate on the trapping column for 10 min to wash away any contaminants. Upon switching inline with the MS, a linear gradient from 95% to 40% solvent A developed for 40 minutes, and in the following 5 minutes the composition of mobile phase was increased to 20% A before decreasing to 95% A for a 15 minute equilibration before the next sample injection. MS data were acquired automatically using Analyst QS 1.0 software Service Pack 8 (ABI MDS SCIEX, Concord, Canada). An information-dependent acquisition method consisting of a 1 second TOFMS survey scan of mass range 400-1200 amu and two 2.5 second product ion scans of mass range 100-1500 amu was followed. The two most intense peaks over 20 counts, with charge state 2-5 were selected for fragmentation, and a 6 amu window was used to prevent the peaks from the same isotopic cluster from being fragmented again. Once an ion was selected for MS/MS fragmentation, it was put on an exclude list for 180 seconds. Curtain gas was set at 23, nitrogen was used as the collision gas and the ionization tip voltage used was 2700V. If the observed A_{215} was greater than 0.1 for any fraction collected during the SCX a 2.5 hour gradient (95-50% solvent A) was used to compensate for the higher peptide concentration in that fraction.

For phosphopeptide identification, 50 μg of phosphorylated DosR was trypsin digested and enriched for phosphopeptides using titanium dioxide matrix then subjected to LC-MS/MS analysis.

Data Analysis – Data files were processed using the Paragon™ algorithm integrated in the ProteinPilot 2.0.1 software (Applied Biosystems/MDS Sciex) in the default search mode with iTRAQ-labeled peptide as sample type, trypsin as the digestion agent, methyl methanethiosulfonate for cysteine modification and QSTAR ESI as the instrument with the thorough search mode applied. The Paragon™ algorithm and the Pro Group™ processing algorithm in the ProteinPilot software were used for peptide identification and isoform-specific quantification and the iTRAQ peak area data were normalized for loading error by auto-biased corrections calculated using the ProteinPilot software. A total of 27063 spectra were analysed against the *M. tuberculosis* proteome (a total of 3924 sequences). ProteinPilotTM also performed protein grouping to remove redundant hits and comparative quantifications using iTRAQ ratios. The Protein and Peptide Summary results obtained from the ProteinPilot software were exported to Microsoft Excel.

The unused protein score represents the sum of the log confidence contributions of unique peptides used exclusively in the identification of the given protein and therefore was unused, not linked, to any other higher ranking protein(s). The total protein score includes all peptide evidence used in the identification of the given protein (unused protein score) and additional peptide evidence that is shared with a higher ranking protein and therefore used in the identification of the higher ranked protein. Thus, same peptides are not assigned repeatedly to different proteins. ProteinPilot software calculates an unused score of 2 for a peptide with 99% identity confidence, and an unused score of 1.3 for a peptide with 95% confidence level. An unused score of > 2 for which only one peptide is listed in the "Peptides(95%)" column, indicates that a minimum of two peptides, one peptide with >95% confidence plus at least one other peptide with less than 95% confidence, were used exclusively for the identification of that protein. Within a protein group of highly homologous proteins (identical peptides), peptides are arbitrarily assigned to one protein for which an unused score and iTRAQ ratio is determined. Other proteins in the group with no additional peptide evidence therefore have an unused protein score of 0. The %Cov(95) is calculated by dividing the number of amino acids of peptides identified with 95% confidence by the total number of amino acids in the protein. Relative quantification was performed on MS/MS scans and

denotes the ratio of the areas under the peaks at 115 Da and 114 Da (untreated Δ*pknH*/WT) and 117 Da and 116 Da (nitrite-treated Δ*pknH*/WT) in this experiment.

Cloning – Construction of pJC8: The multiple cloning region of pALACE (including AflII and PacI restriction sites) and the upstream His_{6x}-tag was amplified using primers J31 (to introduce a BglII restriction site upstream of the amplicon) and S205 (downstream of an internal XhoI site). The amplicon was cut with *Bgl*II and *Xho*I and ligated into the compatible *BamH*I/*Xho*I cut pGEV2, resulting in pJC8.

Construction of pJC10: A portion of the acetamidase promoter including the internal HindIII site (ACET) was amplified from pALACE using primers J85 and J86 to introduce a KpnI restriction site downstream of the translational start site. The N_{Trp} fragment was amplified from PL240 with primers J83 and J84 to introduce flanking KpnI and AflII restriction sites. Three-way ligation was performed with pALACE cut with *Hind*III and *Afl*II, ACET cut with *Hind*III and *Kpn*I, and N_{Trp} cut with *Kpn*I and *Afl*II. The resulting plasmid retained the AflII, NdeI, PacI, and ClaI multi-cloning site from the pALACE vector. Inserts (*cfp-10*, *pknH401, dosR,* $dosR_{T198ET205E}$ $dosR_{145\text{-}217}$, $dosR_{145\text{-}217\ T198ET205E}$) were cloned between AflII and ClaI.

Construction of pJC11: The C_{Trp} fragment was amplified from PL242 with primers J81 and J82 to introduce flanking ClaI and KpnI restriction sites. The entire acetamidase promoter and downstream region was excised from pALACE using *Xba*I and *Cla*I. Three-way ligation was performed with pPE207 cut with *Xba*I and *Kpn*I, the excised acetamidase promoter, and C_{Trp} cut with *Cla*I and *Kpn*I. The resulting plasmid acquired the BamHI, AflII, NdeI, PacI, and ClaI multi-cloning site from the pALACE vector. Inserts (*esat-6*, *dosR*, $dosR_{T198AT205A}$, $dosR_{145\text{-}217\ T198ET205E}$, $dosR_{145\text{-}217}$, $dosR_{145\text{-}217\ T198ET205E}$) were cloned between AflII and ClaI.

SUPPLEMENTAL FIGURE LEGENDS

Fig. S1. MS/MS fragmentation spectrum of DosR phosphopeptides. Spectrum and table of daughter ions identified (bold) for Thr198 phosphorylation *in vitro (A)*, Thr205 phosphorylation *in vitro (B)*, Thr198 phosphorylation *in vivo (C)*, Thr205 phosphorylation *in vivo (D)*, and Thr198 and Thr205 diphosphorylation *in vivo* (*E*, table only).

Fig. S2. Hydrolytic stability of phosphorylated DosR. DosR was phosphorylated by PknH, separated by SDS-PAGE, and transferred onto a PVDF membrane. PVDF strips containing PknH and DosR bands were treated with HCl, NaOH, or ddH_2O. Acid stability and base sensitivity is indicative of Ser/Thr/Tyr phosphorylation and not Asp phosphorylation.

Fig. S3. Transcriptional analysis of DosR regulon genes. Quantitative RT-PCR analyis comparing WT and Δ*pknH* cDNA levels normalized to *sigA* gene expression ± SEM. Cultures of *M. tuberculosis* were treated for 4 h with the indicated inducer. Panels *A*-*F*, showing WT and Δ*pknH* gene expression levels correspond to the Δ*pknH* / WT ratios in columns 1-6 of Fig. 6A, respectively.

Plasmids	**Characteristics**	**Source/Ref.**
Kinase Assays		
pET22b	Produces C-term His_6-tagged proteins, *Amp*	Novagen
pET30b	Produces C-term His_6-tagged proteins, *Kan*	Novagen
pXW13-2	pET22b carrying *dosR* cloned between *Nde*I and *Hind*III, *Amp*	This study
pJC9dosR	pET30b carrying *dosR* cloned between *Nde*I and *Hind*III, *Kan*	This study
pGEX-4T3	Produces N-term GST-tagged proteins, *Amp*	GE Healthcare
pJC6pknH	pGEX-4T3 carrying $pknH_{1-402}$ cloned between *Bam*HI and *Xho*I, *Amp*	This study
pGEV2	Produces N-term G-protein tagged proteins, *Amp*	(50)
pJC8	Derivative of pGEV2, produces G-protein - His_{6x}-tagged proteins, *Amp*	This study
pXW 33-2	pJC8 carrying $dosS_{378-578}$ cloned between *Afl*II and *Pac*I, *Amp*	This study
Split-Trp Assay		
PL240	Produces N_{Trp} fusion proteins, P_{hsp60}, *Gent*	(18)
PL242	Integrative, produces C_{Trp} fusion proteins, P_{dnaK}, *Hyg*	(18)
pALACE	Produces N-term His_6-tagged proteins, $P_{acetamidase}$, *Hyg*	(52)
pPE207	Apramycin resistant mycobacterial shuttle vector, *Apr*	(53)
pJC10	Derivative of pALACE, produces N_{Trp} fusion proteins, *Hyg*	This study
pJC11	Derivative of pPE207, produces C_{Trp} fusion proteins, with $P_{acetamidase}$ from pALACE, *Apr*	This study
pJC10-*cfp10*	pJC10 carrying *cfp10* between *Afl*II and *Cla*I, *Hyg*	This study
pJC10-*pknH*	pJC10 carrying $pknH_{1-402}$ between *Afl*II and *Cla*I, *Hyg*	This study
pJC10-$dosR_{T198ET205E}$	pJC10 carrying full-length $dosR_{T198ET205E}$ between *Afl*II and *Cla*I, *Hyg*	This study
pJC10-*dosR*-C	pJC10 carrying $dosR_{145-217}$ between *Afl*II and *Cla*I, *Hyg*	This study
pJC10-*dosR*-$C_{T198ET205E}$	pJC10 carrying $dosR_{145-217\ T198ET205E}$ between *Afl*II and *Cla*I, *Hyg*	This study
pJC11-*esat6*	pJC11 carrying *esat-6* between *Afl*II and *Cla*I, *Apr*	This study
pJC11-*dosR*	pJC11 carrying full-length *dosR* between *Afl*II and *Cla*I, *Apr*	This study
pJC11-$dosR_{T198AT205A}$	pJC11 carrying full-length $dosR_{T198AT205A}$ between *Afl*II and *Cla*I, *Apr*	This study
pJC11-$dosR_{T198ET205E}$	pJC11 carrying full-length $dosR_{T198ET205E}$ between *Afl*II and *Cla*I, *Apr*	This study

pJC11-*dosR*-C	pJC11 carrying $dosR_{145\text{-}217}$ between *Afl*II and *Cla*I, *Apr*	This study
pJC11-*dosR*-$C_{T198ET205E}$	pJC11 carrying $dosR_{145\text{-}217\ T198ET205E}$ between *Afl*II and *Cla*I, *Apr*	This study
M-PFC Assay		
pUAB100	P_{hps60}-*BamHI*-GCN4-*ClaI*-Gly-mDHFR-[F1,2], *Hyg*	(19)
pUAB200	P_{hps60}-*MfeII*-GCN4-*ClaI*-Gly-mDHFR-[F3], *Kan*	(19)
pUAB300	P_{hps60}-mDHFR-[F1,2], *Hyg*	(19)
pUAB400	P_{hps60}-mDHFR-[F3], *Kan*	(19)
pKP366	pUAB100 carrying *dosR* cloned between *Bam*HI and *Cla*I, *Hyg*	This study
pKP369	pUAB200-carrying $pknH_{1\text{-}401}$ cloned between *Mfe*I and *Cla*I, *Kan*	This study

Cloning primers	**Sequence**	**Restriction Site**
Kinase Assays		
S183 dosR F	CATCACTCATATGAAGGTCTTCTTGGTCGATGACCACG	NdeI
S185 dosR R	TCTCAAGCTTTGGTCCATCACCGGGTGGCC	HindIII
pGEX-PknH F	CATCAGGATCCATGAGCGACGCACAGGACT	BamHI
pGEX-PknH R	GCGACTCGAGGGCCACGGGTTGGTTTTGC	XhoI
J31 pALACE-His F	TTCGAGATCTCACCACCACCACCACCACATC	BglII
S205 pALACE R	CAAACGAGGGGATTACACATGACCAACT	
J51 dosS201 F	GTAGCTTAAGATGCGCGAACTCGACGTACT	AflII
J52 dosS201 R	GACGTTAATTAAGCCGGAAGAGCTACTGCGAC	PacI
Split-Trp Assay		
J81 Ctrp F	TAGTATCGATGGCTCCGGCTCCGGTGGAAAGAG	ClaI
J82 Ctrp R	GCAGGGTACCTAAGGCTTACCGCTTCCTTTCTTAGC	KpnI
J83 Ntrp F	GGACGGTACCATGTACCCATACGATGTTCCAG	KpnI
J84 Ntrp R	GATGCTTAAGGCCTGATCCAGATCCGCCTC	AflII
J85 Acet F	GAACTCAACCTCGCCGTCCTGC	
J86 Acet R	CTGAGGTACCCGATCCCGAATGGTCGACGC	KpnI
J77 dosR F	CGAGCTTAAGGTGGTAAAGGTCTTCTTGGTCGATGAC	AflII
J117 $dosR_{145\text{-}217}$ F	CGACCTTAAGATGGACCCGCTATCAGGCCTTAC	AflII

J87 dosR NOstop R	GTAGATCGATTGGTCCATCACCGGGTGGC	ClaI
J114 dosR stop R	GTTGTTATCGATGTCATGGTCCATCACCGGGTGGCC	ClaI
J89 pknH F	GCAGCTTAAGATGAGCGACGCACAGGACTCG	AflII
J90 pknH stop R	CTACATCGATCACGGGTTGGTTTTGCGCGGGGTCTG	ClaI
ESX_Trp_Fwd	ACATTCCTTAAGATGACAGAGCAGCAGTGG	AflII
ESX_Trp_Rev_NS	ACACACATCGATTGCGAACATCCCAGTGACG	ClaI
CFP10_Trp_Fwd	ACACACCTTAAGATGGCAGAGATGAAGACCG	AflII
CFP10_Trp_Rev	ACACACATCGATTCAGAAGCCCATTTGCGAGG	ClaI
M-PFC Assay		
S616_DosR_100F	ACACAGATCTAGTGGTAAAGGTCTTCTTGGTCGATG	BglII
S615_DosR_100R	TCTCAACGTTTGGTCCATCACCGGGTGG	AclI
S617_PknH-200F	TCTACAATTGTGAGCGACGCACAGGACTC	MfeI
S618_PknH-200R	TCTTATCGATTGCCGGGTTGGTTTTGCGCGG	ClaI

Mutagenesis primers

DosR T198A F	TGGGCATGGAACGTCGGGCGCAAGCCGC
DosR T198A R	GCGGCTTGCGCCCGACGTTCCATGCCCA
DosR T205A F	GCGGTATTCGCGGCGGAGTTGAAGCG
DosR T205A R	CGCTTCAACTCCGCCGCGAATACCGC
DosR T198ET205E F	GAACGTCGGGAGCAAGCCGCGGTATTCGCGGAGGAGTTGAAGC
DosR T198ET205E R	GCTTCAACTCCTCCGCGAATACCGCGGCTTGCTCCCGACGTTC

qRT-PCR primers	Forward	Reverse
sigA	CTCGGTTCGCGCCTACCTCA	GCGCTCGCTAAGCTCGGTCA
rv0079	CCGCAAACCGGTCGTGCTAA	TCCAGCCCGATAGACCACAG
rv0574c	CTTGAGAACACCGCGACCGA	CACGTTATCCGGGTGCATCC
rv1737c	CGTGTTCGGTATGGGCATGG	GATGGCGTGGGTGGTGAACAG
rv1738	CGACATATCGATCGACGAAC	GCCAACACCCACCAATTCCT
rv2005c	CGATGCGGCGATGAGGAACA	CCTCGTCCTCCTGCCAAACC
rv2031c, hspX	ATGGCCACCACCCTTCCCGTT	TGTCGAAGGTGGGCCGGAGT

rv2032, acg	TTTACGCGACCGACCACTCC	CGCCAGATGCAAAGGATCGT
rv2623	CGACGCACTCAAGGTGGTTGAA	GTGGATGATCACGACCGGACAG
rv2627c	ACGTCCGGTCAGCAATCATC	AAATCCGCTAGGCTTCTCCA
rv2628	GATGTGGTCGGATAGGCAGGT	CCTGATAGATGGTGGCGGATTG
rv3128c	GTGTGTTGGAGTTTGGGCGTGA	TCTTTGGCCTTCGCGGTCTT
rv3131	CCCTCCATCCACAACACGCA	CAATGCCACACCACAGCTGA
rv3133c, dosR	CCGACCGAATGTTCCTAGCC	TCAACTCCGTCGCGAATACC

EMSA oligos

DosR Box Dist T	GGCAGACAACAGGGTCAATGGTCCCCAAGTGGATCA
DosR Box Dist C	GGTGATCCACTTGGGGACCATTGACCCTGTTGTCTG
HspX CP up	GACGGGCGCGGACAAATGGCCCGCGCTTCGGGGACTTCTGTCCCTAGCCCTGG
HspX CP dn	GCCAGGGCTAGGGACAGAAGTCCCCGAAGCGCGGGCCATTTGTCCGCGCCCGT

Table S1. Plasmids, primers, and oligonucleotide sequences. *Amp,* ampicillin resistance; *Kan*, kanamycin resistance; *Gent*, gentamycin resistance; *Hyg*, hygromycin resistance; *Apr*, apramycin resistance; *P*, promoter.

Excel File:

Table S2. iTRAQ analysis of Δ*pknH*/WT ratios for untreated and $NaNO_2$ treated samples.

Figure S1

A Thr198 *in vitro* phosphorylation

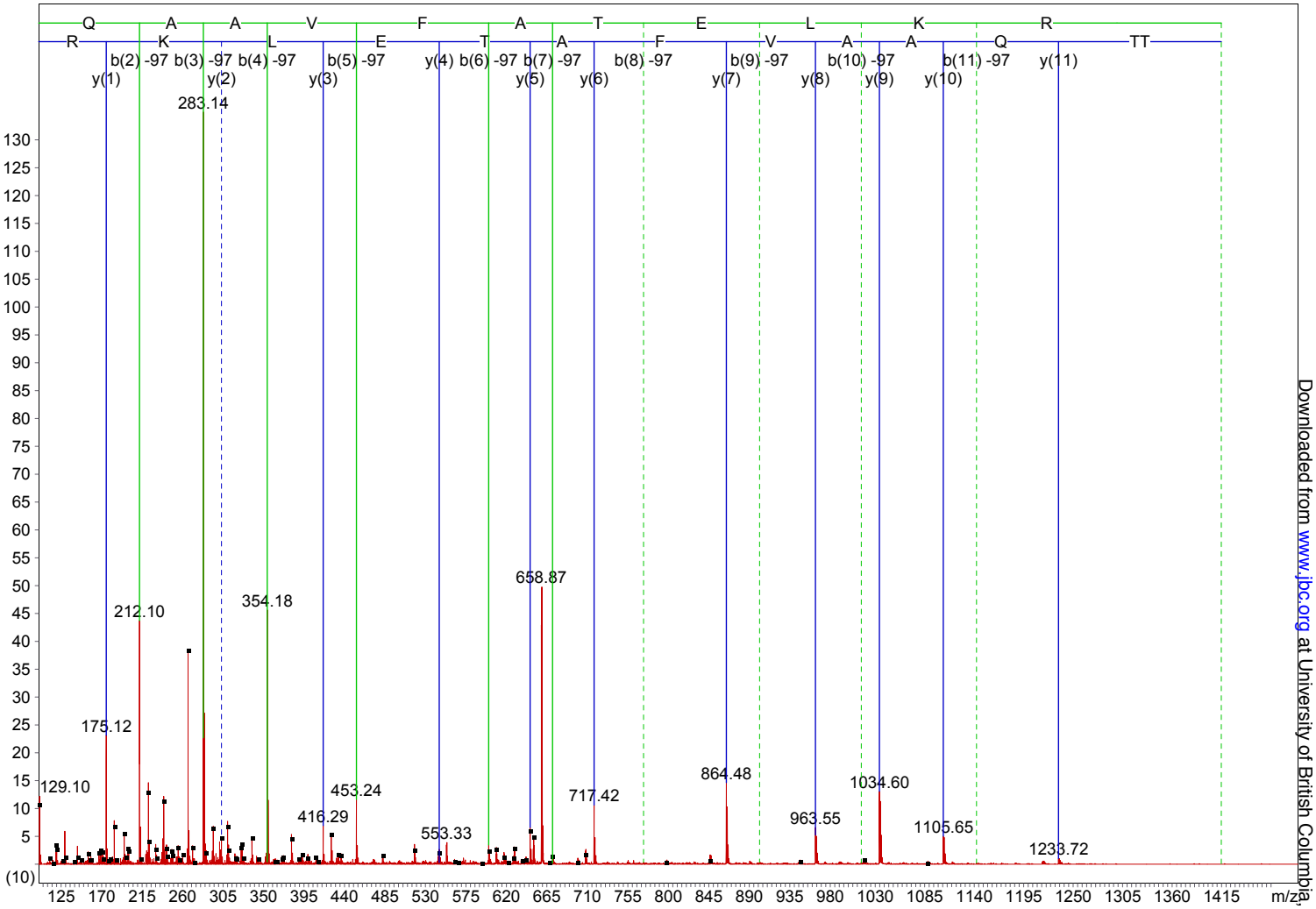

General

Precursor MW:	1413.6766	Precursor Charge:	2
Mass tolerance:	0.06 Da	N-terminal Modification:	(none)
Cysteine Modification:	(none)	C-terminal Modification:	(none)
Methionine Modification:	(none)	Digest Agent:	Trypsin
Present AAs:	(none specified)	Missing AAs:	(none specified)

Fragment Ions

Mass Type:	Monoisotopic	m/z Tolerance:	0.06 Da
Minimum Intensity:	0.1% of tallest peak		

Peptide Sequence Results: (none)

Partial Sequence Tag Results: (none)

Matches: 18
Hypertag: (none) BQAAVFATELKR -0.0251 (none)
Ion Charge: 1
Fragments:

Residue	Mass	a	b	b-H3PO4	b-NH3	y	y-H2O	y-H3PO4	y-NH3
B, PhT	181.0140	154.0264	182.0213	84.0444	164.9947	1414.7090	1396.6984	1316.7321	1397.6825
Q, Gln	128.0586	282.0849	***310.0799***	***212.1030***	293.0533	1233.6950	1215.6844	1135.7181	1216.6684
A, Ala	71.0371	353.1221	381.1170	***283.1401***	364.0904	***1105.6364***	1087.6259	1007.6595	1088.6099
A, Ala	71.0371	424.1592	452.1541	***354.1772***	435.1275	***1034.5993***	1016.5887	936.6224	1017.5728
V, Val	99.0684	523.2276	551.2225	***453.2456***	534.1960	***963.5622***	945.5516	***865.5853***	946.5356
F, Phe	147.0684	670.2960	698.2909	600.3140	681.2644	***864.4938***	***846.4832***	766.5169	847.4672
A, Ala	71.0371	741.3331	769.3280	671.3511	752.3015	***717.4254***	699.4148	619.4485	700.3988
T, Thr	101.0477	842.3808	870.3757	772.3988	853.3492	***646.3883***	628.3777	548.4114	629.3617
E, Glu	129.0426	971.4234	999.4183	901.4414	982.3918	***545.3406***	527.3300	447.3637	528.3140
L, Leu	113.0841	1084.5075	1112.5024	1014.5255	1095.4758	***416.2980***	398.2874	318.3211	399.2714
K, Lys	128.0950	1212.6024	1240.5973	1142.6204	1223.5708	***303.2139***	285.2034	205.2370	***286.1874***
R, Arg	156.1011	1368.7035	1396.6984	1298.7215	1379.6719	***175.1190***	157.1084	77.1421	158.0924

B Thr205 *in vitro* phosphorylation

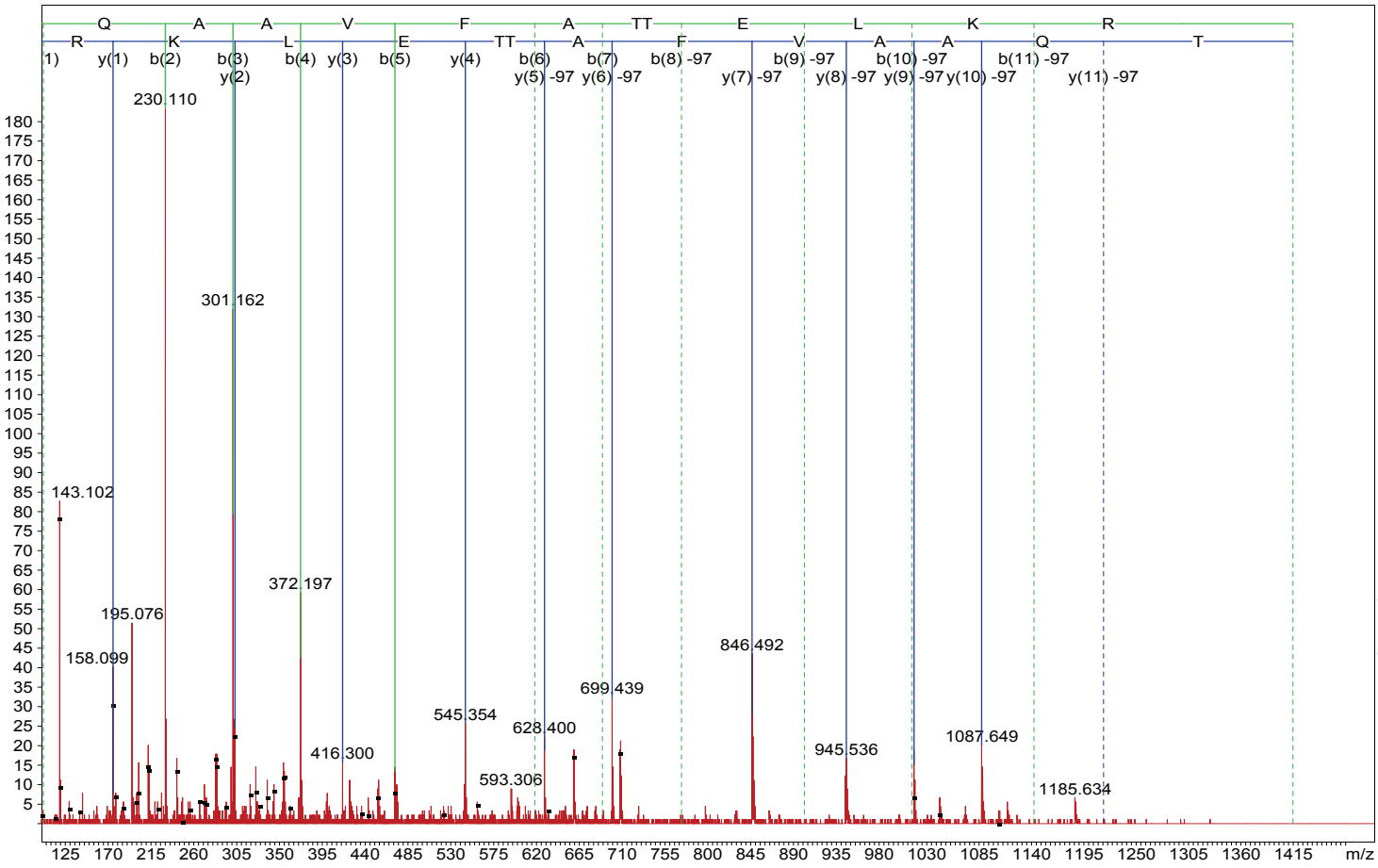

General

Precursor MW:	1413.7196	Precursor Charge:	2
Mass tolerance:	0.06 Da	N-terminal Modification:	(none)
Cysteine Modification:	(none)	C-terminal Modification:	(none)
Methionine Modification:	(none)	Digest Agent:	Trypsin
Present AAs:	(none specified)	Missing AAs:	(none specified)

Fragment Ions

Mass Type:	Monoisotopic	m/z Tolerance:	0.06 Da
Minimum Intensity:	0.1% of tallest peak		

Peptide Sequence Results: (none)

Partial Sequence Tag Results: (none)

Matches: 28
Hypertag: (none) TQAAVFABELKR 0.0179 (none)
Ion Charge: 1
Fragments:

Residue	Mass	Immonium	a	b	b-H2O	b-NH3	y	y-H3PO4
T, Thr	101.0477	74.0600	74.0600	102.0550	84.0444	85.0284	1414.7090	1316.7321
Q, Gln	128.0586	101.0709	***202.1186***	***230.1135***	***212.1030***	***213.0870***	1313.6613	1215.6844
A, Ala	71.0371	44.0495	273.1557	***301.1506***	***283.1401***	***284.1241***	1185.6028	***1087.6259***
A, Ala	71.0371	44.0495	***344.1928***	***372.1878***	***354.1772***	***355.1612***	***1114.5656***	***1016.5887***
V, Val	99.0684	72.0808	443.2613	***471.2562***	***453.2456***	***454.2296***	***1043.5285***	***945.5516***
F, Phe	147.0684	120.0808	590.3297	618.3246	600.3140	601.2980	***944.4601***	***846.4832***
A, Ala	71.0371	44.0495	661.3668	689.3617	671.3511	672.3352	797.3917	***699.4148***
B, PhT	181.0140	154.0264	842.3808	870.3757	852.3651	853.3492	726.3546	***628.3777***
E, Glu	129.0426	102.0550	971.4234	999.4183	981.4077	982.3918	***545.3406***	447.3637
L, Leu	113.0841	86.0964	1084.5075	1112.5024	1094.4918	1095.4758	***416.2980***	318.3211
K, Lys	128.0950	101.1073	1212.6024	1240.5973	1222.5868	1223.5708	***303.2139***	205.2370
R, Arg	156.1011	***129.1135***	1368.7035	1396.6984	1378.6879	1379.6719	***175.1190***	77.1421

C Thr198 *in vivo* phosphorylation

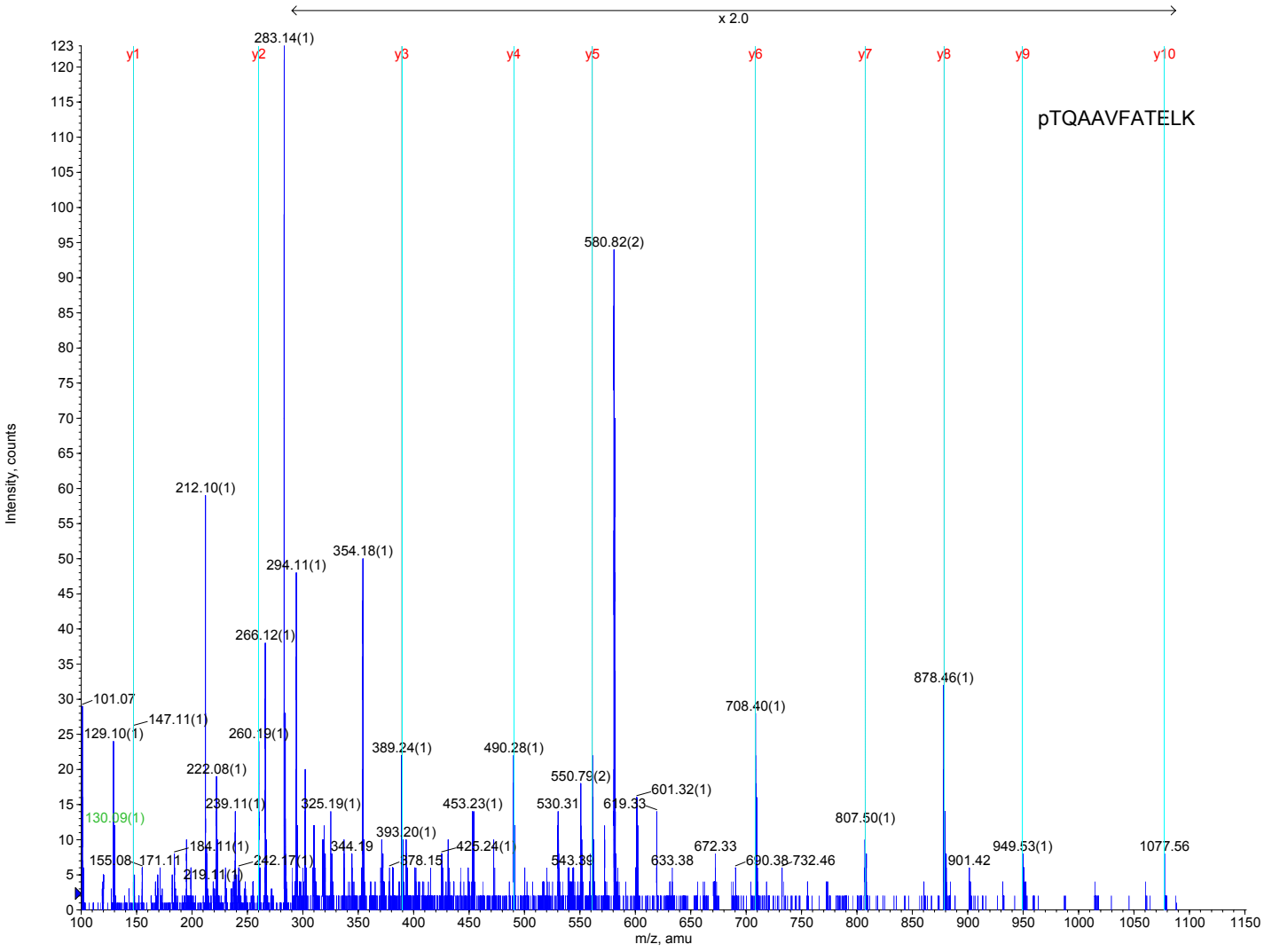

General

Precursor MW:	1257.8998	Precursor Charge:	2
Mass tolerance:	0.06 Da	N-terminal Modification:	(none)
Cysteine Modification:	(none)	C-terminal Modification:	(none)
Methionine Modification:	(none)	Digest Agent:	Trypsin
Present AAs:	(none specified)	Missing AAs:	(none specified)

Fragment Ions

Mass Type:	Monoisotopic	m/z Tolerance:	0.06 Da
Minimum Intensity:	0.1% of tallest peak		

Peptide Sequence Results: (none)

Partial Sequence Tag Results: (none)

Matches: 25
Hypertag: (none) BQAAVFATELK 0.2992 (none)
Ion Charge: 1
Fragments:

Residue	Mass	Immonium	a	b	b-H3PO4	y	y-NH3
B, PhT	181.0140	154.0264	154.0264	182.0213	84.0444	1258.6079	1241.5813
Q, Gln	128.0586	***101.0709***	282.0849	***310.0799***	***212.1030***	1077.5939	1060.5673
A, Ala	71.0371	44.0495	***353.1221***	***381.1170***	***283.1401***	***949.5353***	932.5088
A, Ala	71.0371	44.0495	424.1592	452.1541	***354.1772***	***878.4982***	861.4716
V, Val	99.0684	72.0808	523.2276	551.2225	***453.2456***	***807.4611***	790.4345
F, Phe	147.0684	***120.0808***	670.2960	698.2909	600.3140	***708.3927***	691.3661
A, Ala	71.0371	44.0495	741.3331	769.3280	671.3511	***561.3243***	***544.2977***
T, Thr	101.0477	74.0600	842.3808	870.3757	772.3988	***490.2871***	473.2606
E, Glu	129.0426	***102.0550***	971.4234	999.4183	***901.4414***	***389.2395***	***372.2129***
L, Leu	113.0841	86.0964	1084.5075	1112.5024	1014.5255	***260.1969***	***243.1703***
K, Lys	128.0950	***101.1073***	1212.6024	1240.5973	1142.6204	***147.1128***	***130.0863***

D Thr205 *in vivo* phosphorylation

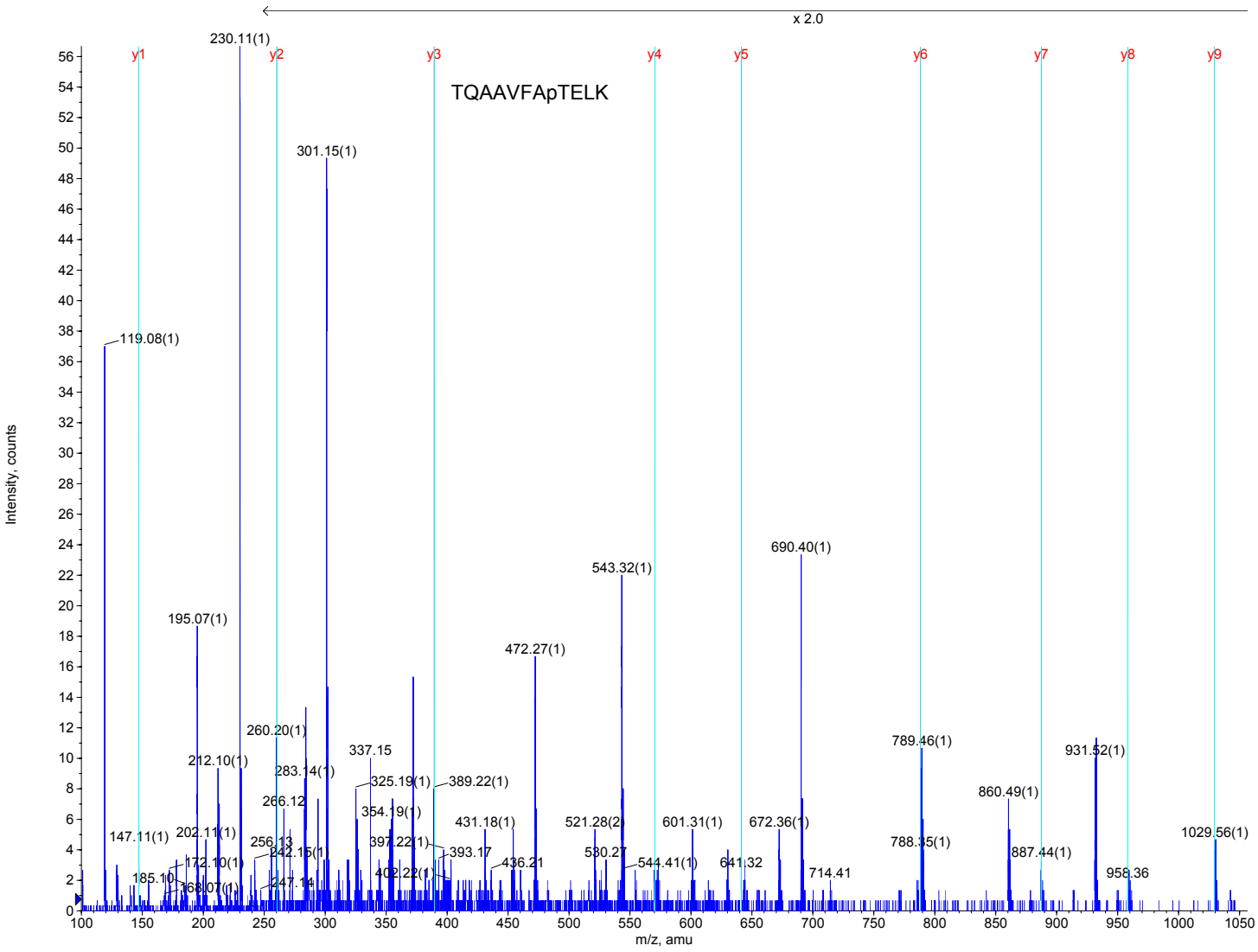

General

Precursor MW:	1257.6090	Precursor Charge:	2
Mass tolerance:	0.06 Da	N-terminal Modification:	(none)
Cysteine Modification:	(none)	C-terminal Modification:	(none)
Methionine Modification:	(none)	Digest Agent:	Trypsin
Present AAs:	(none specified)	Missing AAs:	(none specified)

Fragment Ions

Mass Type:	Monoisotopic	m/z Tolerance:	0.06 Da
Minimum Intensity:	0.1% of tallest peak		

Peptide Sequence Results: (none)

Partial Sequence Tag Results: (none)

Matches: 42
Hypertag: (none) TQAAVFABELK 0.0084 (none)
Ion Charge: 1
Fragments:

Residue	Mass	Immonium	a	a-NH3	b	b-H2O	b-NH3	y	y-H3PO4
T, Thr	101.0477	74.0600	74.0600	57.0335	102.0550	84.0444	85.0284	1258.6079	1160.6310
Q, Gln	128.0586	***101.0709***	***202.1186***	***185.0921***	***230.1135***	***212.1030***	***213.0870***	1157.5602	1059.5833
A, Ala	71.0371	44.0495	***273.1557***	***256.1292***	***301.1506***	***283.1401***	***284.1241***	***1029.5016***	***931.5247***
A, Ala	71.0371	44.0495	***344.1928***	***327.1663***	***372.1878***	***354.1772***	***355.1612***	***958.4645***	***860.4876***
V, Val	99.0684	72.0808	***443.2613***	***426.2347***	***471.2562***	***453.2456***	***454.2296***	***887.4274***	***789.4505***
F, Phe	147.0684	***120.0808***	590.3297	***573.3031***	618.3246	600.3140	***601.2980***	***788.3590***	***690.3821***
A, Ala	71.0371	44.0495	661.3668	***644.3402***	689.3617	671.3511	***672.3352***	***641.2906***	***543.3137***
B, PhT	181.0140	154.0264	842.3808	825.3542	870.3757	852.3651	853.3492	***570.2535***	***472.2766***
E, Glu	129.0426	102.0550	971.4234	954.3968	999.4183	981.4077	982.3918	***389.2395***	291.2626
L, Leu	113.0841	86.0964	1084.5075	1067.4809	1112.5024	1094.4918	1095.4758	***260.1969***	162.2200
K, Lys	128.0950	***101.1073***	1212.6024	1195.5759	1240.5973	1222.5868	1223.5708	***147.1128***	49.1359

E Thr198 Thr205 *in vivo* diphosphorylation (Table)

General

Precursor MW:	1493.6893	Precursor Charge:	2
Mass tolerance:	0.06 Da	N-terminal Modification:	(none)
Cysteine Modification:	(none)	C-terminal Modification:	(none)
Methionine Modification:	(none)	Digest Agent:	Trypsin
Present AAs:	(none specified)	Missing AAs:	(none specified)

Fragment Ions

Mass Type:	Monoisotopic	m/z Tolerance:	0.06 Da
Minimum Intensity:	0.1% of tallest peak		

Peptide Sequence Results: (none)

Partial Sequence Tag Results: (none)

Matches: 46
Hypertag: (none) BQAAVFABELKR 0.0212 (none)
Ion Charge: 1
Fragments:

Residue	Mass	Immonium	a	a-NH3	b	b-H3PO4	b-NH3	y	y-H3PO4	y-NH3
B, PhT	181.0140	***154.0264***	***154.0264***	136.9998	182.0213	84.0444	164.9947	1494.6753	1396.6984	1477.6488
Q, Gln	128.0586	***101.0709***	282.0849	265.0584	***310.0799***	***212.1030***	293.0533	1313.6613	***1215.6844***	1296.6348
A, Ala	71.0371	44.0495	353.1221	336.0955	***381.1170***	***283.1401***	***364.0904***	***1185.6028***	***1087.6259***	1168.5762
A, Ala	71.0371	44.0495	424.1592	407.1326	***452.1541***	***354.1772***	***435.1275***	***1114.5656***	***1016.5887***	1097.5391
V, Val	99.0684	72.0808	***523.2276***	506.2010	***551.2225***	***453.2456***	***534.1960***	***1043.5285***	***945.5516***	1026.5020
F, Phe	147.0684	***120.0808***	***670.2960***	653.2695	***698.2909***	***600.3140***	681.2644	***944.4601***	***846.4832***	927.4336
A, Ala	71.0371	44.0495	741.3331	724.3066	769.3280	***671.3511***	752.3015	***797.3917***	***699.4148***	780.3651
B, PhT	181.0140	***154.0264***	922.3471	905.3206	950.3420	852.3651	933.3155	***726.3546***	***628.3777***	***709.3280***
E, Glu	129.0426	***102.0550***	1051.3897	1034.3632	1079.3846	981.4077	1062.3581	***545.3406***	447.3637	***528.3140***
L, Leu	113.0841	86.0964	1164.4738	1147.4472	1192.4687	1094.4918	1175.4421	***416.2980***	318.3211	***399.2714***
K, Lys	128.0950	***101.1073***	1292.5687	1275.5422	1320.5637	1222.5868	1303.5371	***303.2139***	205.2370	***286.1874***
R, Arg	156.1011	***129.1135***	1448.6699	1431.6433	1476.6648	1378.6879	1459.6382	***175.1190***	77.1421	***158.0924***

Figure S2

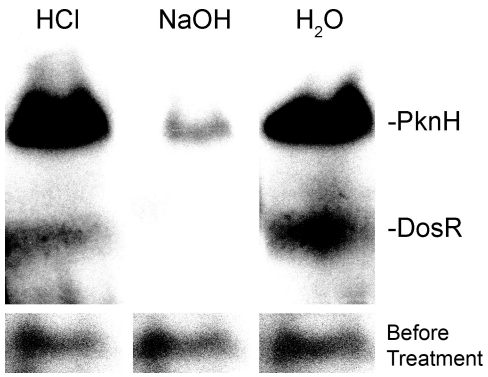

Figure S3